Assessing Mechanisms Behind Crossmodal Associations between Visual Textures and Temperature Concepts

Francisco Barbosa Escobar[1, 2], Carlos Velasco[3], Derek V. Byrne[1], and Qian Janice Wang[1,2]

[1] Department of Food Science, Faculty of Technical Sciences, Aarhus University

[2] Department of Food Science, Faculty of Science, University of Copenhagen

[3] Centre for Multisensory Marketing, Department of Marketing, BI Norwegian Business School

Author Note

Francisco Barbosa Escobar https://orcid.org/0000-0003-1784-451X

Carlos Velasco https://orcid.org/0000-0002-4864-2315

Derek V. Byrne https://orcid.org/0000-0001-6715-2306

Qian Janice Wang https://orcid.org/0000-0001-7054-2137

Preprint, data, scripts, preregistrations, and additional materials are openly available on the project's Open Science Framework page (https://osf.io/g2vmy/). We have no conflicts of interest to disclose. This research was supported by a Carlsberg Foundation Young Researcher Fellowship received by Qian Janice Wang (CF19-0587).

Correspondence concerning this article should be addressed to Francisco Barbosa Escobar, Department of Food Science, Faculty of Science, University of Copenhagen, Rolighedsvej 26, 1958 Frederiksberg C, Denmark. Email: francisco.escobar@food.ku.dk.

This paper has been accepted for publication in *J Exp Psychol Hum Percept Perform*.

Abstract

In the last decades, there has been a growing interest in crossmodal correspondences, including those involving temperature. However, only a few studies have explicitly examined the underlying mechanisms behind temperature-related correspondences. Here, we investigated the relative roles of an underlying affective mechanism and a semantic path (i.e., regarding the semantic knowledge related to a single common source identity or meaning) in crossmodal associations between visual textures and temperature concepts using an associative learning paradigm. Two online experiments using visual textures previously shown to be associated with low and high thermal effusivity (Experiment 1) and visual textures with no consensual associations with thermal effusivity (Experiment 2) were conducted. Participants completed a speeded categorisation task before and after an associative learning task, in which they learned mappings between the visual textures and specific affective or semantic stimuli related to low and high temperatures. Across the two experiments, both the affective and semantic mappings influenced the categorisation of visual textures with the hypothesized temperatures, but there was no influence on the reaction times. The effect of learning semantic mappings was larger than that of affective ones in both experiments, suggesting that a semantic path has more weight than an affective mechanism in the formation of the associations studied here. The associations studied here could be modified through associative learning establishing correlations between visual textures and either affective or semantic stimuli.

Keywords: crossmodal correspondences, temperature, affect, semantic congruency.

Public Significance Statement

We show that associative learning can give rise to new crossmodal associations between visual textures and temperature concepts. Furthermore, our results demonstrate that an associative learning paradigm involving affective and semantic stimuli can reverse individuals' previous associations.

https://doi.org/10.1037/xhp0001131

https://doi.org/10.1037/xhp0001131

Assessing Mechanisms Behind Crossmodal Associations between Visual Textures and Temperature Concepts

Crossmodal correspondences are often surprising associations people have between attributes in different sensory modalities (Spence, 2011, 2020c). Throughout the years, the literature has uncovered multiple correspondences involving different senses and types of features, although most studies have tended to focus on the visual and auditory domains (Parise & Spence, 2012; Spence, 2020c). Even though many crossmodal correspondences have been uncovered, the mechanisms giving rise to them are not fully understood (Parise, 2016), and hence the origins of crossmodal correspondences are still a matter of debate (Turoman et al., 2018). Nevertheless, the literature so far has put forward four non-mutually exclusive and potentially complementary explanations that can help explain the existence of crossmodal correspondences, namely the statistical, structural, lexical, and affective-mediation accounts (Spence, 2011). According to the statistical account, crossmodal correspondences originate from the internalisation of natural statistics in the environment (Ernst, 2007; Parise et al., 2014), and most crossmodal correspondences seem to stem from this account (Spence, 2011, 2018, 2020c). The structural account suggests that some correspondences come from common neural encoding of the dimensions of stimuli, as more intense sensory stimuli are represented by more intense neural firing (Stevens, 1957; Walsh, 2003). The lexical account poses that correspondences may come from the use of the same adjectives or terms to describe different types of sensory stimuli (Martino & Marks, 1999, 2000, 2001). Finally, the affective account suggests that people associate different stimuli because they evoke the same affective or emotional associations (Palmer et al., 2013).

In the last decades, researchers have increasingly been studying crossmodal correspondences involving temperature (see Spence, 2020b for a review). Recently, crossmodal correspondences between visual textures and temperature concepts were uncovered (Barbosa Escobar et al., 2022a). Visual textures relate to the two-dimensional representations of the patterns of elements that describe the surface characteristics of objects or materials (American Psychological Association, n.d.; Klatzky & Lederman, 2010). Associations between visual textures and temperature concepts seem to be based on the thermal effusivity of materials (i.e., their ability to exchange thermal energy with their environment; Cottrill et al., 2018), as the latter determines how cold or hot materials feel to the touch (Wongsriruksa et al., 2012). Furry visual textures are associated with higher temperatures (i.e., related to materials with lower thermal effusivity) and that crystalline visual textures are associated with lower temperatures (i.e., related to materials with higher thermal effusivity). As Spence (2020d) suggested, temperature-based correspondences likely come from the internalisation of environmental statistics. This seems to be the case for crossmodal correspondences between visual textures and temperature. As Barbosa Escobar et al. (2022a) suggested, these associations may come from the internalisation of statistical regularities between temperature and material properties, and consequently visual textures, as individuals tend to see objects and textures before touching them and perceiving their temperature. In this case, materials and material properties co-occur in the environment. Hence, people develop associations between specific (visual) textures and different temperatures due to the material properties of objects with these textures. Moreover, many people seem to think of a specific entity to develop these associations, which stem from regular exposure to these entities and their statistical regularities. An affective account may also play a role in forming these associations, as tactile and visual textures on the one hand and temperature on the other, may evoke similar affective reactions (Barbosa Escobar et al., 2022a). However, all these accounts seem to be tightly interrelated and hard to separate from each other.

In the present research, we aimed to investigate further the mechanisms behind the recently uncovered crossmodal associations between visual textures and temperature. Two online experiments using an associative learning paradigm together with speeded categorisation tasks were conducted to examine the relative influence of an affective mechanism and a semantic path in the formation of these crossmodal associations. In the first experiment, visual textures with consensual associations with temperature concepts were used, whereas in the second experiment, visual textures without such associations were used. While a few studies have used learning tasks to explicitly induce or change crossmodal associations (Ernst, 2007; Flanagan et al., 2008), here a learning paradigm involving mappings of stimuli related to two different underlying paths (i.e., affective, semantic), instead of directly learning the exact crossmodal associations per se (i.e., mappings between the specific stimuli/dimensions) were used. This work thus contributes to the academic literature on crossmodal correspondences by explicitly studying the underlying mechanisms of a novel set of crossmodal associations while helping reduce the gap in the knowledge related to i) how crossmodal correspondences originate and ii) the relative strength of these different underlying mechanisms. Moreover, the present research to the literature by investigating whether new crossmodal associations can be formed through associative learning involving visual textures on one side and affective and semantic stimuli on the other.

Theoretical Background and Hypotheses Development

Affective Mechanism

Textures (tactile and visual) and temperature can evoke diverse emotional responses (Etzi et al., 2016; Iosifyan & Korolkova, 2019). An emotional mediation account may partially explain

https://doi.org/10.1037/xhp0001131

associations between visual textures and temperature, as they can share similar affective influences. Temperature is tightly linked to emotions, as evidenced by the multiple bidirectional causal effects between them. On the one hand, different temperatures can influence emotional states (Noelke et al., 2016), and on the other hand, individuals' skin temperature increases or decreases in response to changes in emotional states (Rimm-Kaufman & Kagan, 1996). Moreover, emotions can affect people's ambient temperature perception and thermal comfort (Wang & Liu, 2020). Relevant to the present study, people from different countries tend to consistently associate specific temperature concepts with particular emotions (Barbosa Escobar et al., 2021). The latter authors found that people associate temperatures of 0° and 10 °C with negatively valenced, low arousal emotions; temperatures of 20 °C with positively valenced, low-to-medium arousal emotions; and temperatures of 30 °C with positively valenced, high-arousal emotions, respectively. However, temperatures of 40 °C are associated with high-arousal and either positively or negatively valenced emotions.

Visual textures contain critical information for identifying surfaces and materials (Motoyoshi et al., 2007), and they guide expectations about the properties of tactile stimuli (Spence, 2020c). In this way, visual textures evoke associations corresponding to the tactile textures they may represent. Previous research has found that individuals associate different tactile textures with different emotions (Essick et al., 2010; Etzi et al., 2014, 2016; Iosifyan, 2020; Iosifyan & Korolkova, 2019). For instance, Iosifyan and Korolkova (2019) investigated associations between 21 different tactile textures (e.g., granite, leather, fur, marble, concrete) and six specific emotion categories, namely happiness, fear, disgust, anger, surprise, and sadness. The authors found that individuals associated different felt textures with different emotion categories. Furthermore, Etzi et al. (2016) found that different material (e.g., smoothness) and affective (e.g., pleasantness, comfort) properties of tactile surfaces (e.g., cotton, satin, tinfoil, sandpaper, abrasive sponge) were associated with words describing emotional states (e.g., sadness, happiness, anger, among others). Moreover, visual textures themselves provide information that triggers emotional expectations and responses (Liu et al., 2018).

Crossmodal associations between different visual textures and different temperature concepts may arise if they evoke similar emotional connections. For instance, a furry visual texture may evoke positive emotional associations, such as happiness, as it can be regarded as soft and cosy (Kergoat et al., 2012). Hence, since furry visual textures and high temperatures share associations with positive emotions, this can lead to mappings between visual textures and temperature.

Semantic Path

The associations between visual textures and temperature concepts studied here may lie somewhere in the broad spectrum of crossmodal associations (Barbosa Escobar et al., 2021). This spectrum encompasses semantic congruency at one end and crossmodal correspondences at the other (Chen & Spence, 2017; Parise, 2016). Semantic congruency refers to pairs of stimuli tied to the same source identity or meaning (Chen & Spence, 2010), such as the sight of a dog coupled with the sound of a dog (e.g., a bark; Chen & Spence, 2010; Hein et al., 2007). At the other end of the spectrum, crossmodal correspondences refers to links between low-level features of different sensory modalities (Parise & Spence, 2013; Spence, 2011). While temperature is a low-level feature, visual textures are relatively complex stimuli that can relate to specific materials. Thus, associations between visual textures and temperature are not strictly crossmodal correspondences. Moreover, as visual textures may bring to mind specific origin materials, the associations studied here may be closer to semantic congruency. That said, it is also uncertain whether the distinction between crossmodal correspondences and semantic congruency is continuous or more discrete (Parise, 2016).

Semantic congruency is often confounded with crossmodal correspondences that emerge from the use of the same lexicon or adjectives to talk about different dimensions of multisensory experiences, which stem from the semantic coding hypothesis originally developed by Martino and Marks (1999, 2000, 2001). These latter correspondences are sometimes confusingly referred to as semantic correspondences or semantically mediated correspondences. To avoid any confusion, following the suggestion of Walker (2016) and later Spence (2022), these latter correspondences originally derived from the semantic coding hypothesis (Martino & Marks, 1999, 2000, 2001) are referred to as lexical correspondences.

It is possible that the crossmodal associations studied here emerge from semantic knowledge related to a common source identity based on experience. Examples of associations based on a source object can be found in colour-odour associations, such as those between the colour yellow and the odour of bananas, where the source object is the banana fruit (Spence & Levitan, 2021; see Spence, 2020a for a review). Better accuracy in determining the source of an odour is related to more consistent matches with colours (de Valk et al., 2017; Goubet et al., 2018). In our case, people may form associations based on their knowledge or experience of the perceived temperature of the material/object that the visual texture evokes. Here, individuals may be drawing from the semantic knowledge of a source (visual) texture and its material properties (e.g., thermal effusivity) that affect how it feels to the touch (Bergmann Tiest & Kappers, 2009; Blaine, 2018).

https://doi.org/10.1037/xhp0001131

Associative Learning and Crossmodal Correspondences

The origin of crossmodal correspondences and how they develop throughout people's lives are still a matter of discussion. It is possible that some correspondences are innate or that at least they develop some days after birth (20 – 30 days; Lewkowicz & Turkewitz, 1980). Other correspondences are learned in time through the internalisation of the statistical regularities of the environment, and others can be semantically mediated. Indeed, research has shown that crossmodal correspondences can be generated experimentally through associative learning paradigms (see Parise, 2016; Spence, 2022). This shows that crossmodal correspondences have at least some degree of plasticity. As Parise (2016) suggested, experience can influence mappings of sensory cues (within and across modalities) and create new mappings in adults. Moreover, individuals can learn new mappings between sensory cues based on statistical co-occurrence in a single training session (e.g., Brunel et al., 2015; Ernst, 2007; Huang et al., 2022; Kaliuzhna et al., 2015; Knoeferle et al., 2016).

In the present work, we started from the extant literature showing that most (if not all) crossmodal correspondences, in particular those that are temperature-based, originate from a statistical account and our previous results in line with this (Barbosa Escobar et al., 2022a). Furthermore, we build on the work of Ernst (2007) and the literature on associative learning and crossmodal correspondences to investigate the relative influence of an affective mechanism and a semantic path (i.e., semantic knowledge related to a single common source identity) in crossmodal associations between visual textures and temperature concepts. It is worth highlighting that research on the interaction between semantic congruency and crossmodal correspondences is scarce. Here an associative learning paradigm to create mappings between specific visual textures and either affective or semantic stimuli related to temperature concepts was used. In this way, mapping a visual texture with a stimulus congruent with a specific underlying mechanism (e.g., affective, semantic) would be expected to result in a stronger crossmodal association between the visual texture and a temperature concept. For example, if the underlying mechanism was an affective one, affective-based learning would be expected to result in a stronger temperature association. Here, visual textures previously found to be crossmodally associated with low (i.e., *crystalline*) and high (i.e., *furry*) temperature concepts were used. Visual textures with no consensual temperature associations (i.e., *wrinkled*, *stained*) were also used since this would provide an additional robust measure of the relative strength of the different mechanisms, as there are no pre-existing biases to overcome. To measure the crossmodal associations and their strength, a speeded categorisation task before and after the learning paradigm was used. In the speeded categorisation task, participants categorised, as rapidly as possible, visual textures as either hot or cold.

Informed by literature on the affective and semantic content of both visual textures and temperature, as well as the proposed mechanisms behind crossmodal correspondences, we expected that the mappings between visual textures and affectively or semantically related stimuli with temperature concepts would lead individuals to associate the given visual textures with the corresponding temperature concept more often (higher probability) and more rapidly (lower reaction time). More formally, in the case of visual textures that have been previously found to be associated with different temperature concepts, we hypothesised that:

H_{1A}: Participants will classify the *furry* (vs. *crystalline*) visual texture as hot (vs. cold) more often after exposure to the affective congruent mappings than to the incongruent ones.

H_{1B}: Participants will classify the *furry* (vs. *crystalline*) visual texture as hot (vs. cold) more often after exposure to the semantic congruent mappings than to the incongruent ones.

H_{2A}: Participants will classify the visual textures more rapidly after being exposed to the affective congruent mappings than to the incongruent ones.

H_{2B}: Participants will classify the visual textures more rapidly after being exposed to the semantic congruent mappings than to the incongruent ones.

Furthermore, based on the results of our previous study suggesting that people think of a specific entity to arrive at the associations studied here (Barbosa Escobar et al., 2022a), we expected that the semantic path would have a higher weight in explaining these correspondences relative to the affective account. More formally, we hypothesised that:

H_{3A}: The effect of the semantic congruent mappings on the categorisation responses will be greater than the effect of the affective mappings.

H_{3B}: Learning congruent semantic mappings would result in lower reaction times compared to the congruent affective mappings.

In the case of visual textures with no consensual temperature associations, we expected that the affective and semantic mappings would lead to more frequent crossmodal associations with the corresponding hypothesised temperature concepts. More formally, we hypothesised that:

H_{4A}: Participants will classify a visual texture as hot (vs. cold) more often when it is mapped to the affective stimuli related to high (vs. low) temperatures than when it is mapped to affective stimuli related to low (vs. high) temperatures.

https://doi.org/10.1037/xhp0001131

H_{4B}: Participants will classify a visual texture as hot (vs. cold) more often when it is mapped to the semantic stimuli related to high (vs. low) temperatures than when it is mapped to affective stimuli related to low (vs. high) temperatures.

However, in the case of visual textures with no consensual crossmodal associations with temperature concepts, we did not expect to see any difference in reaction times, as these textures, as a group, do not have any consistent emotional or semantic associations.

Experiment 1

Experiment 1 was designed to test the influence of an affective mechanism and a semantic path in the formation of crossmodal associations between visual textures and temperature concepts. To do this, an associative learning paradigm and speeded categorisation tests to assess the degree of visual texture-temperature associations before and after learning were used. In this experiment, visual textures with consensual associations to temperature concepts were used to evaluate a base scenario in which the associations already existed and examine the extent to which they could be strengthened or weakened. As Spence (2022) suggested, there are multiple ways to measure the strength of crossmodal correspondences, and the most prevalent one lies in the general agreement in the population studied, which can range from about chance level (~ 50%) to near perfect agreement. Here, we quantified the strength of the associations by modelling the level of agreement about the correspondences, as measured by the probability that a given visual texture would be categorised as either hot or cold.

Methods

Transparency and Openness

We report how the required sample sizes were determined, all data cleaning methods, all manipulations, and all measures in the studies, following JARS (Kazak, 2018). The two studies

https://doi.org/10.1037/xhp0001131

reported here were preregistered. All data, analysis script, research materials, and preregistrations are available at the project's Open Science Framework (OSF) page (https://osf.io/g2vmy/). Required sample sizes were calculated using G*Power (Faul et al., 2007), and all the data were analysed using R, version 4.0.1 (R Core Team, 2021).

Participants

The required sample size was determined via a power analysis based on goodness-of-fit test using G*Power (Faul et al., 2007). We aimed to have at least 280 participants in total to obtain a power of .80, using a medium effect size of Cohen's W = .3 with an alpha level of .05. A total of 300 native English speakers from the UK (143 females, 152 males, 5 unreported), aged 18 – 41 years (M_{age} = 28.90 years, SD_{age} = 6.11) took part in the experiment. Participants were recruited from Prolific (https://www.prolific.co/) and received GBP 1.20 for their participation. To increase the quality of the pool of participants, we pre-screened for participants who had an approval rate of at least 98% in Prolific. The experiments complied with the World Medical Association's Declaration of Helsinki, and before starting the experiment, all participants provided their informed consent to take part in them. As simple online experiments that consisted of an associative learning exercise and categorisation of stimuli similar to those found in everyday life (i.e., artistic representations of naturalistic visual textures and emoji expressions) and did not pose any harm, the studies complied with the policies and requirements stated by the Aarhus University Research Ethics Committee and were therefore exempted from the need of formal ethical approval.

Apparatus and Materials

For the visual textures stimuli, we selected the two visual textures most strongly associated with low- and high-temperature concepts from (Barbosa Escobar et al., 2022a), which

https://doi.org/10.1037/xhp0001131

were extracted from the Describable Textures Dataset (DTD; Cimpoi et al., 2014). The *matted* (associated with high temperatures) and the *crystalline* (associated with low temperatures) visual textures were selected. To reduce the visual textures' resemblance to specific entities, we applied a pencil sketch filter to them. For the *matted* visual texture, we used the Artificial Intelligence-based website IMAGETOSKETCH (https://imagetosketch.com/), and for the *crystalline* visual texture, we used the *sketch* function of the {sketcher} R package (Tsuda, 2020), as it provided a better quality image. Both visual textures were grayscale and were histogram equalised in Adobe Photoshop 22.1.1. The stimuli for the affective mappings consisted of the facial expressions (i.e., only eyebrows and smile) of two emojis taken from the EmojiGrid (Toet et al., 2018), as in Barbosa Escobar et al. (2022b). The emojis from the EmojiGrid have been specifically created to convey specific values of the valence and arousal dimensions of affect. They are not part of the official Unicode emoji and are not found in people's everyday life in any of the digital communication platforms (e.g., iOS, Android, Facebook). Here, the low valence, low arousal (V1A1; henceforth called sad) and the high valence, low arousal (V5A1; henceforth called happy) emojis were selected, as Barbosa Escobar et al. (2022a) found that visual textures associated with high-temperature concepts tend to exhibit positive valence, whereas those associated with low temperatures tend to exhibit negative valence. As per the stimuli for the semantic mappings (i.e., based on the semantic knowledge related to a single common source identity as per semantic congruency), we aimed to use stimuli related to the indirect associations evoked that lead to temperature associations for the selected visual textures without explicitly creating temperature mappings. Hence, the words *fur* and *metal*, were used based on the findings of Barbosa Escobar et al. (2022a). We selected fur, as it evokes mappings to the warmth of living beings that are, or were, once alive. On the other hand, we selected metal, as it relates to a

https://doi.org/10.1037/xhp0001131

category of materials with overall high thermal effusivity, so keeping physical temperature constant, they feel cold to the touch.

Design and Procedure

The experiment followed a 2 (Mechanism: affective, semantic) × 2 (Pairing: congruent, incongruent) × 2 (Time: before learning, after learning) mixed design, with mechanism and pairing as between-subjects factors and time as within-subject factor. In this way, each participant was randomly assigned to one of the four possible associative learning groups derived from the interaction between mechanism and pairing. Based on the findings of Barbosa Escobar et al. (2022a), in the congruent affective mappings, the *matted* visual texture (henceforth called *furry*) was paired with the happy emoji expression, and the *crystalline* visual texture was paired with the sad emoji expression. In the congruent semantic mappings, the *furry* visual texture was paired with the word *fur*, and the *crystalline* visual texture was paired with the word *metal*. In the incongruent mappings, these pairings were reversed. Figure 1 presents all the possible mappings in the associative learning task. Furthermore, to have a benchmark for each participant, they completed a speeded categorisation task before the associative learning task and another one after it.

Figure 1

Possible Mappings in the Associative Learning Task in Experiment 1

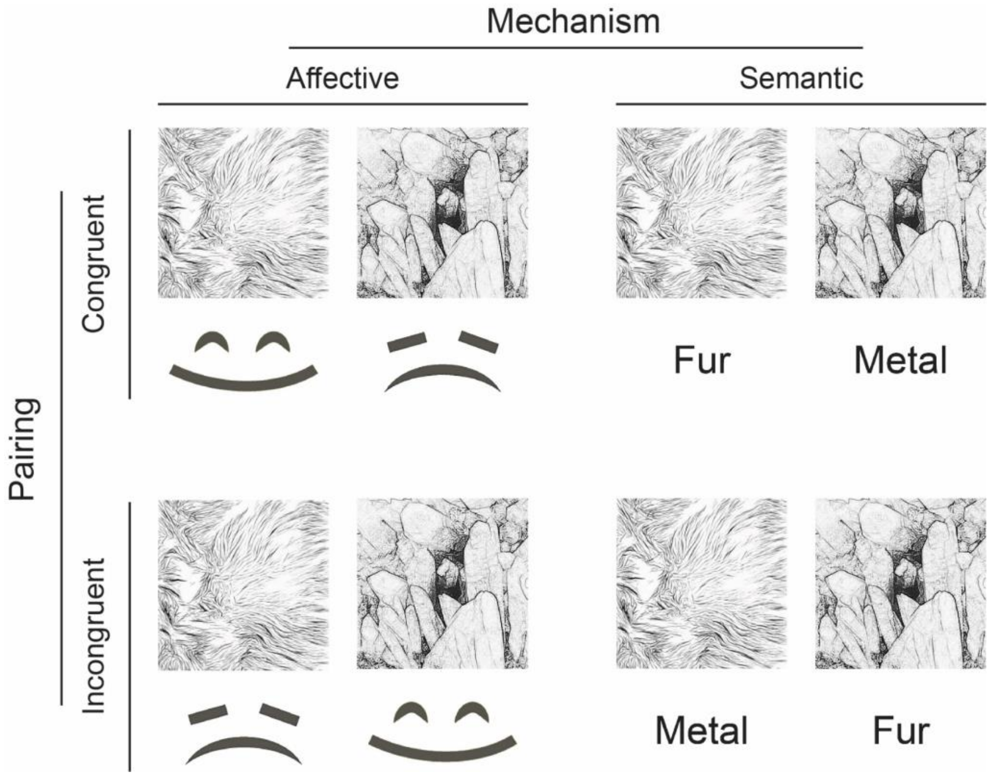

Note. The figure presents the four different mappings in Experiment 1 based on the interaction of mechanism and pairing.

Both experiments presented here were programmed and conducted on Gorilla (https://gorilla.sc/). Participants completed the experiment online using either a desktop or a laptop. The experiment was composed of a self-paced associative learning task and two speeded categorisation tasks (one before and one after the associative learning task). The associative learning task was similar to the one used in Experiment 3 in Knoeferle et al. (2016). The associative learning task comprised a learning phase (five learning blocks) and a testing phase (five testing blocks), alternating between the other. In the learning blocks, each participant was exposed to two mappings, one involving the *furry* visual texture and the other involving the *crystalline* one, presented in random order. More specifically, participants were exposed to a mapping paring each visual texture (*furry* and *crystalline*) with either an affective (sad or happy emoji expression) or a semantic (the word *fur* or *metal*) stimulus. Each learning block was comprised of eight trials (four trials per mapping). Each trial started with a fixation cross in the centre for 500 ms, followed by a 100 ms interstimulus pause. Then, a mapping appeared in random order in the centre of the screen for 3,000 ms. In the testing blocks, participants completed a matching test. Here, they were presented either with a visual texture or with an affective or semantic stimulus in the centre of the screen. Participants were tasked to select the corresponding stimulus based on the previously learned mappings from two possible choices at the bottom of the screen with their mouse. To ensure that participants learned the mappings from the associative learning paradigm regardless of the type of target stimuli presented in the centre of the screen (either a visual texture or an affective/semantic stimulus), in the testing blocks, we included the two possible types of stimuli. In each testing block, each stimulus was presented twice for a total of eight trials. Each trial in the testing blocks started with a fixation cross and an interstimulus pause identical to the learning trials. After a response was given in each testing trial, a response feedback stimulus appeared in the centre of the screen for 200 ms, which consisted of a green checkmark for correct responses or a red “X” for incorrect responses. The allocation of the stimuli (congruent or incongruent) to either the left or right position was counterbalanced. Figure 2 presents a diagram of the experimental design.

Each speeded categorisation task consisted of a total of 20 trials (ten trials for each of the two visual textures). In each trial, participants had to classify, as fast as possible, a visual texture presented in the centre of the screen as either cold or hot by pressing the “F” or the “J” keys on their keyboard, corresponding to the left and right sides of the screen based a specific mapping provided to participants before starting the task. The mapping of the temperature words to the keys remained visible at the bottom of the screen for the duration of each trial. The temperature word assigned to the keys in each speeded categorisation task (before and after the associative learning task) was counterbalanced per participant.

Figure 2

Experimental Procedure of Experiments 1 and 2

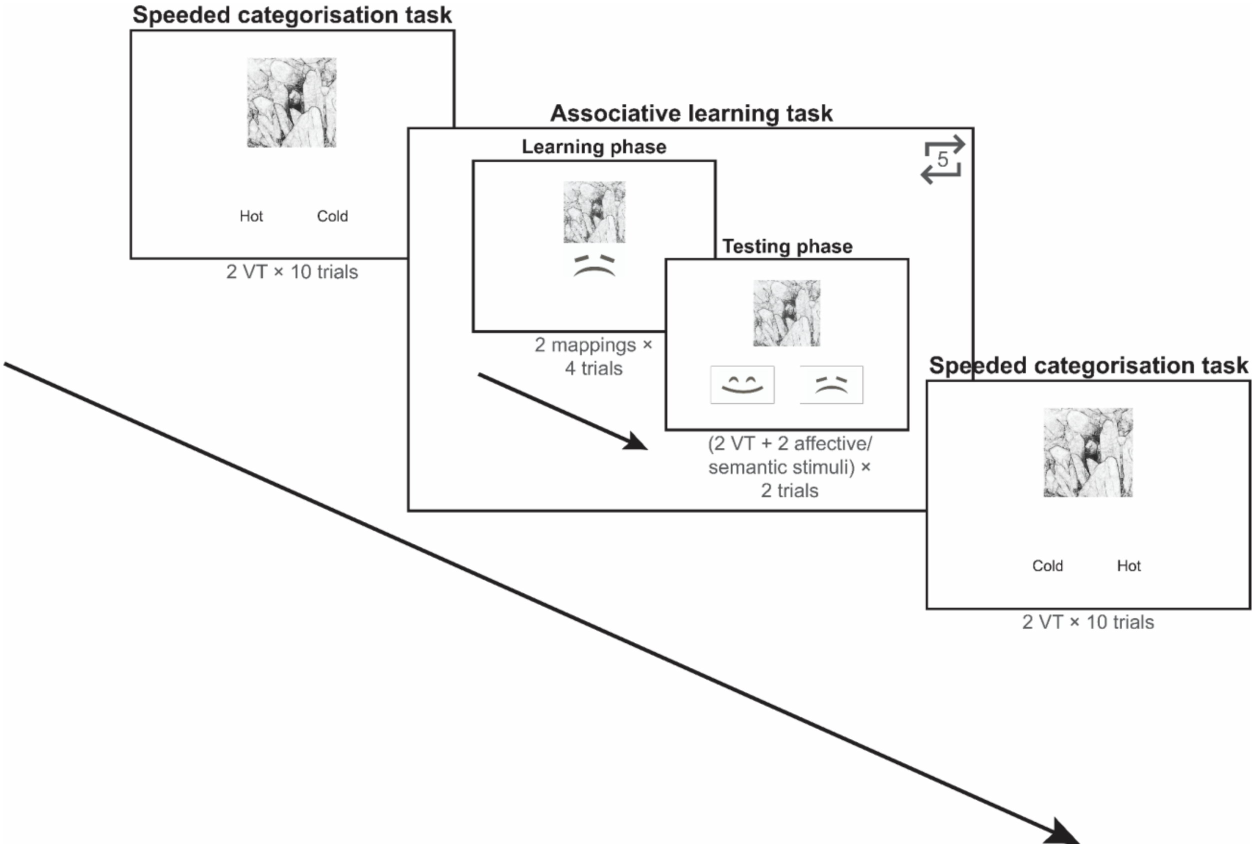

Note. The figure presents a schematic representation of the procedure of Experiments 1 and 2. VT = visual texture.

Before starting the experiment, participants were presented with an overall description of the experiment and then provided their informed written consent. Then, participants completed

https://doi.org/10.1037/xhp0001131

the first speeded categorisation task. Afterwards, participants were assigned to one of the four possible groups derived from the interaction of mechanism and pairing, and they completed the associative learning task introduced as a memory test. Afterwards, they completed the second categorisation task. Finally, they completed a set of demographic questions (i.e., age, gender).

Data Analysis

Two response measures from the experiment were obtained, namely categorisation responses and reaction times (RT). All analyses were conducted in R (R Core Team, 2021). First, to obtain an overall perspective of participants' categorisation of the two visual textures under the different conditions before and after the associative learning task, we conducted a log-likelihood ratio goodness of fit test (G^2) with Williams' correction as per the *GTest* function of the {DescTools} R package (Signorell, 2021). We visualized the proportion of categorisation via mosaic plots. Subsequently, as we were interested in the visual textures previously found to be crossmodally associated with low- and high-temperatures being classified as such, we performed separate logistic Generalized Linear Mixed Models (GLMMs) for each visual texture to investigate the probability that they were classified as hot (for the *furry* visual texture) and as cold (for the *crystalline* visual texture). The independent variables for the GLMMs were selected based on the study design and included the three factors. More specifically, we specified the interaction of mechanism, pairing, and time as fixed effects and participant's ID as random effect. These models would allow us to evaluate the effect of the two mechanisms on the change in probabilities before and after the associative learning task, as well as the difference between the congruent and incongruent mechanisms after the associative learning task. The GLMMs were performed via the *glmer* function of the {lme4} R package (Bates et al., 2015). Each GLMM was tested via Likelihood Ratio Tests (LRTs) against its corresponding null model consisting only of

https://doi.org/10.1037/xhp0001131

participants' IDs as random effect. In addition, the Akaike information criterion (AIC) for each model was computed. Subsequently, we analysed statistically significant differences of the estimated probabilities derived from the model by conducting Bonferroni-corrected pairwise comparisons via the *emmeans* function of the {emmeans} R package (Lenth, 2021). Furthermore, we evaluated the explanatory power of the models using the pseudo-R^2 method suggested by Zhang (2017) using the *rsq.glmm* function of the {rsq} R package (Zhang, 2022).

As per RTs, we identified and treated outliers by winsorizing values more than three median absolute deviations (MADs) plus or minus the median for each participant. More specifically, any value that was three MADs above or below the median was replaced with the median value plus or minus three times the MAD, respectively. We used the MAD, as it is a robust measure to identify the spread of the data (Leys et al., 2013, 2019). To analyse RTs, we first fit a GLMM with Gamma distribution and identity link function on RT with the interaction of time, mechanism, and pairing as fixed effect and with participant ID and visual texture as random effects. We specified a Gamma distribution with untransformed data, as it effectively models reaction time data and is intuitive to interpret (Lo & Andrews, 2015). Specifically, the Gamma distribution closely approximate reaction time data, which is positively skewed and bounded on the left by zero. In addition, the mixed effects are able to model the multilevel structure of the data and hence permit the analysis of trial-level data, instead of requiring averaging across participants, which increases statistical power (Lo & Andrews, 2015). Furthermore, through the random effects, the model considers idiosyncratic differences of participants. As suggested by Lo and Andrews (2015), effects greater than two standard deviations (i.e., $|t| > 2$) were considered to be significant at the .05 level. Furthermore, to probe the effects of each mechanism on each of the visual textures, we fit two separate GLMMs on RT with Gamma distributions and identity link functions for each mechanism, with the interaction of visual texture, time, and pairing as fixed effect and with participant ID as random effect. Each GLMM was tested via LRTs against their respective null model including only the participant's ID as random effect. Then Bonferroni-corrected pairwise comparisons were performed. Furthermore, as with the logistic GLMM, we computed pseudo-R^2s for each model to evaluate the influence of each mechanism.

Results

To corroborate that participants indeed learned the mappings between the visual textures and either the affective or semantic stimuli, we verified their performance in the testing phase of the associative learning task. The results showed that participants obtained a high percentage of correct responses in the associative learning task (M = 97.6%, SD = 5.3%) showing that participants learned the mappings. Out of the 300 participants, 182 participants scored 100%. Only six participants scored less than 80% of correct responses. There were no significant differences in the percentage of correct responses between the affective and the semantic mappings, $F(1, 298) = 1.52$, $p = .219$, $\eta_p^2 = .005$; $M_{semantic}$ = 97.9%, $SD_{semantic}$ = 4.1% vs. $M_{affective}$ = 97.2%, $SD_{affective}$ = 6.2%. However, participants responded slightly faster to the semantic mappings than the affective ones in the associative learning task, $F(1, 298) = 10.50$, $p = .001$, $\eta_p^2 = .034$; $M_{semantic}$ = 1,502 ms, $SD_{semantic}$ = 469.74 vs. $M_{affective}$ = 1676 ms, $SD_{affective}$ = 461.15.

Categorisation Responses

The log-likelihood ratio goodness of fit tests revealed that there was a significant association between all the factors (i.e., mechanism, pairing, time) for the *furry*, $G^2(15)$ = 1,108.70, $p < .001$, and for the *crystalline*, $G^2(15)$ = 3,617, $p < .001$ visual textures. Figure 3 presents the mosaic plots of the categorisation responses for both visual textures. As expected,

https://doi.org/10.1037/xhp0001131

regarding the *furry* visual texture, when participants were exposed to the congruent pairings of both the affective and semantic mechanisms, they classified the visual texture as hot more often after the associative learning task than before. Furthermore, after the congruent semantic and affective mappings, the *furry* visual texture was classified as hot more often than after the respective incongruent pairings for both conditions. Under the incongruent pairing of the affective mechanism, there was no difference in categorisation before and after the associative learning task, although in both instances participants classified the *furry* visual texture as hot more often. What is more, when exposed to the incongruent semantic pairings, participants classified the *furry* visual texture as hot less often after the associative learning task than before, so that the visual texture was classified as cold virtually as often as hot.

Figure 3

Mosaic Plots of Categorisation Responses in Experiment 1

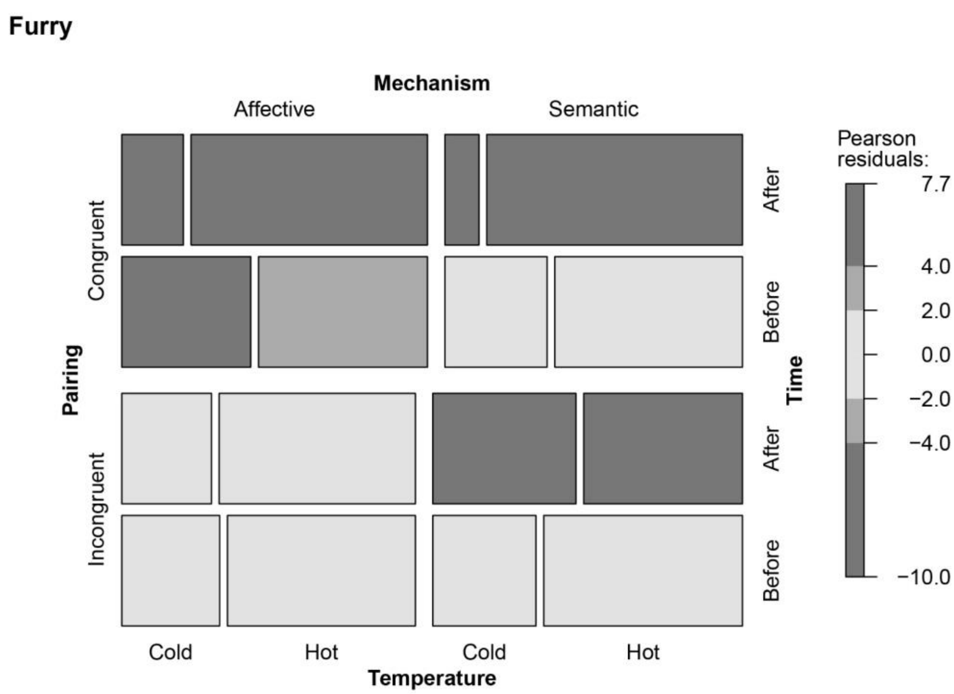

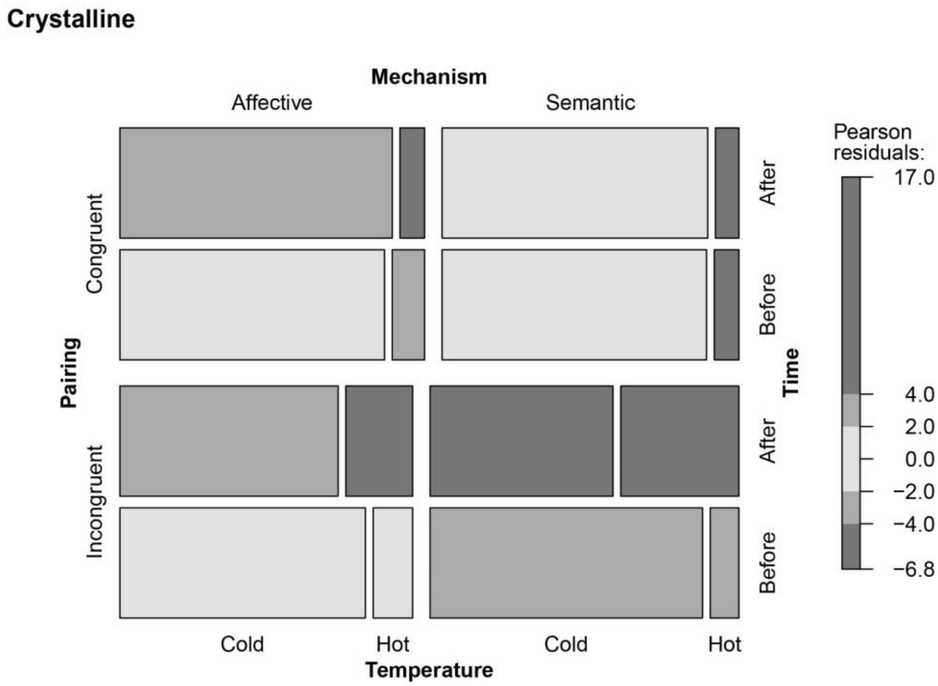

Note. The mosaic plots show the proportion in which each visual texture (*furry* in the upper panel and *crystalline* in the lower panel) was classified as either cold or hot (indicated on the bottom side) before and after the associative learning paradigm (indicated on the left-hand side) comprising the different mechanisms (indicated on the top side) and pairings (indicated on the right-hand side).

As per the *crystalline* visual texture, under the congruent affective pairing, participants classified the visual texture as cold marginally more often after the associative learning task than before, whereas there was no difference under the semantic congruent pairings after compared to before the associative learning task. Nevertheless, participants classified the visual texture as cold more often after the associative learning task with the congruent pairings than after the corresponding incongruent pairings. This was true for both the semantic learning task and the affective learning task. Furthermore, in both the semantic and affective incongruent pairings, the *crystalline* visual texture was classified as cold less often after the associative learning task than before. This effect was more than three times larger for the semantic pairings than the affective ones.

The logistic GLMM involving the *furry* visual texture revealed a significant main effect of time, a significant effect of the two-way interaction between pairing and time, and a significant three-way interaction of mechanism, pairing, and time. Table 1 presents the results of all the logistic GLMMs, and Table 2 presents the results of the models fit analysis, including their corresponding pseudo-R^2s. Figure 4 presents the estimated marginal means deriving from all the logistic GLMM models. Overall, the probability of the *furry* visual texture being classified as hot was significantly higher after the associative learning task (.89, 95% CI = [.84, .93]) than before (.73, 95% CI = [.63, .81]; $p < .001$). As expected, under the congruent pairings, the visual texture had a higher probability of being classified as hot after the associative learning task (.97, 95% CI = [.94, .98]) than before (.66, 95% CI = [.51, .78]; $p < .001$). However, this effect was reversed in the incongruent pairings, as the visual texture had a higher probability of being classified as hot before the associative learning task (.79, 95% CI = [.67, .87]) than after (.71, 95% CI = [.57, .82]; $p < .001$).

https://doi.org/10.1037/xhp0001131

Table 1

Results of the Logistic GLMMs in Experiment 1

	(A) Furry			(B) Crystalline		
	Overall (1)	Affective (2)	Semantic (3)	Overall (4)	Affective (5)	Semantic (6)
Intercept	3.24**	1.12	2.92**	86.89***	120.79***	73.96***
	1.52 – 6.92	0.46 – 2.71	1.55 – 5.51	36.39 – 207.47	45.01 – 324.21	32.84 – 166.57
	(.002)	(.807)	(.001)	(< .001)	(< .001)	(< .001)
$\text{Mechanism}_{\text{Affective}}$	0.35			1.03		
	0.12 – 1.01			0.30 – 3.57		
	(.053)			(.966)		
$\text{Pairing}_{\text{Incongruent}}$	1.2	3.42	1.25	1.5	0.67	1.54
	0.41 – 3.49	0.95 – 12.25	0.51 – 3.07	0.45 – 4.97	0.17 – 2.61	0.50 – 4.73
	(.74)	(.059)	(.623)	(.511)	(.563)	(.454)
$\text{Time}_{\text{After}}$	10.74***	22.13***	10.23***	1.08	1.9*	1.08
	7.31 – 15.80	13.41 – 36.51	7.00 – 14.95	0.68 – 1.72	1.13 – 3.18	0.68 – 1.71
	(< .001)	(< .001)	(< .001)	(.732)	(.016)	(.733)
$\text{Mechanism}_{\text{Affective}} \times \text{Pairing}_{\text{Incongruent}}$	2.64			0.49		
	0.57 – 12.18			0.09 – 2.73		
	(.213)			(.413)		
$\text{Mechanism}_{\text{Affective}} \times \text{Time}_{\text{After}}$	1.82			1.73		
	0.98 – 3.36			0.87 – 3.45		
	(.057)			(.119)		
$\text{Pairing}_{\text{Incongruent}} \times \text{Time}_{\text{After}}$	0.030***	0.07***	0.03***	0.02***	0.11***	0.03***
	0.02 – 0.05	0.04 – 0.12	0.02 – 0.05	0.01 – 0.05	0.06 – 0.22	0.01 – 0.05
	(< .001)	(< .001)	(< .001)	(< .001)	(< .001)	(< .001)
$\text{Mechanism}_{\text{Affective}} \times \text{Pairing}_{\text{Incongruent}} \times \text{Time}_{\text{After}}$	2.56*			4.79**		
	1.18 – 5.58			1.84 – 12.44		
	(.018)			(.001)		
Participants	300	149	151	300	149	151
Observations	6,000	2,980	3,020	6,000	2,980	3,020

Note. The table presents the results of all the logistic GLMMs in Experiment 1. The values for each variable correspond, from top to bottom to its odds ratio, 95% confidence interval, and *p*-value in parentheses. Models 1 – 3 relate to the *furry* visual texture, whereas models 4 – 6 relate to the *crystalline* visual texture. * $p < .05$, ** $p < .01$, *** $p < .001$.

https://doi.org/10.1037/xhp0001131

Table 2

Model Fit Results of Logistic GLMMs in Experiment 1

Model		AIC	LRT			Pseudo-R^2s		
			d	X^2	*p*	R^2_{Model}	$R^2_{Fixed\ Effects}$	$R^2_{Random\ effects}$
Furry - Overall	Participant	4,744.5				.55		
	Mechanism × Pairing × Time	4,281.0	7	477.6	<.001	.63	.05	.57
Furry - Affective	Participant	2,090.0				.62		
	Pairing × Time	1,865.0	3	231	<.001	.7	.03	.67
Furry - Semantic	Participant	2,652.5				.47		
	Pairing × Time	2,408.4	3	250.1	<.001	.55	.08	.48
Crystalline - Overall	Participant	3,277.5				.49		
	Mechanism × Pairing × Time	2,862.8	7	428.8	<.001	.62	.08	.54
Crystalline - Affective	Participant	1,370.3				.58		
	Pairing × Time	1,312.0	3	54.29	<.001	.63	.03	.61
Crystalline - Semantic	Participant	1,905.0				.42		
	Pairing × Time	1,551.2	3	359.9	<.001	.62	.13	.49

Note. The table presents the model fit results of all the logistic GLMMs in Experiment 1 against their corresponding null models. The null models only included participants' IDs. AIC = Akaike information criterion; LRT = Likelihood ratio test.

Figure 4

Estimated Marginal Means from the Logistic GLMM Models in Experiment 1

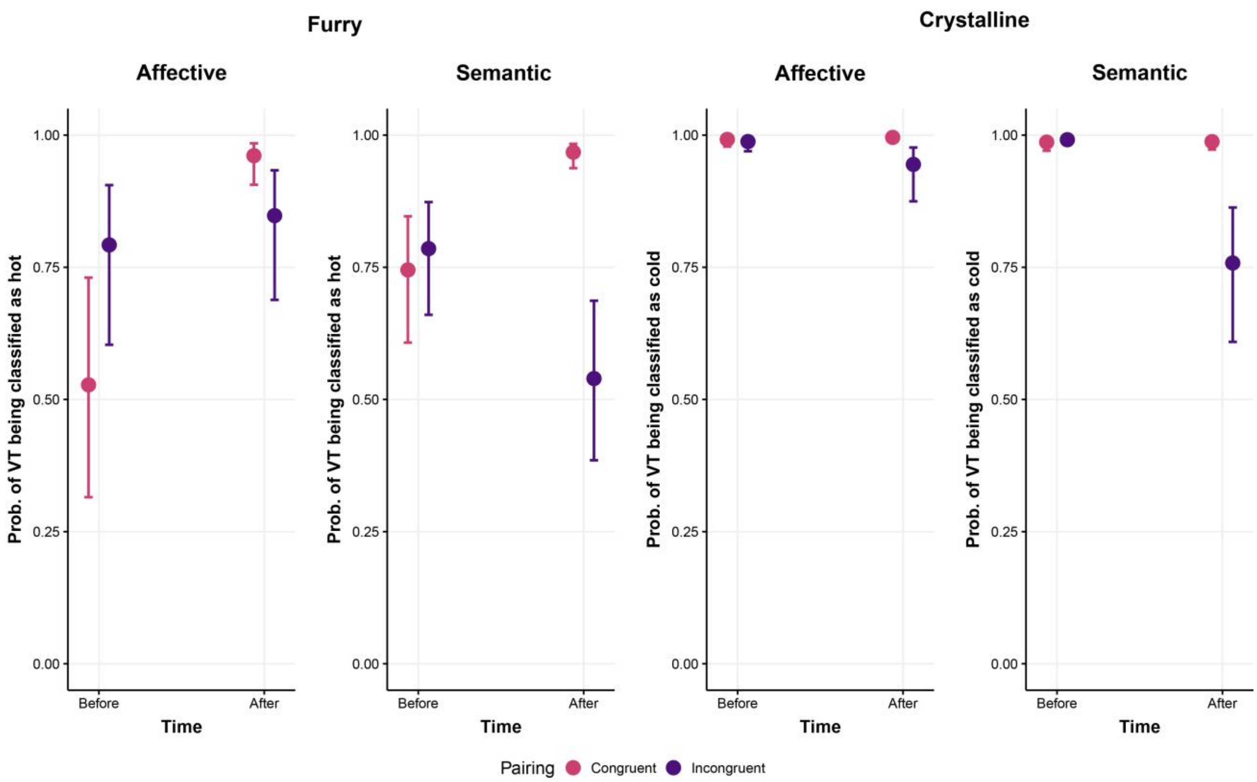

Note. The figure presents the estimated marginal means deriving from all the logistic GLMM models in Experiment 1. The y-axis represents the probability that the visual texture was classified as hot (for the *furry* one) and as cold (for the *crystalline* one). The timing of the speeded categorisation task, before or after the associative learning paradigm, is indicated in the x-axis. Error bars represent the 95% CI resulting from the models. VT = visual texture.

To probe the three-way interaction in the first model involving the *furry* visual texture, we ran two separate GLMMs splitting the data by mechanism. As per the affective mechanism, the results revealed a significant main effect of time and the two-way interaction between pairing and time (Table 1). The probability of the visual texture being classified as hot was significantly

https://doi.org/10.1037/xhp0001131

higher after the associative learning task (.92, 95% CI = [.85, .96]) than before (.67, 95% CI = [.50, .81]; $p < .001$). Under the congruent pairings, the probability was higher after (.96, 95% CI = [.89, .99]) than before (.53, 95% CI = [.29, .76]; $p < .001$) the associative learning task. Surprisingly, under the incongruent pairings, the probability was slightly higher after the associative learning task (.85, 95% CI = [.66, .94]) than before (.79, 95% CI = [.57, .92]; $p = .046$). In terms of the semantic path, the results revealed a significant main effect of time and the two-way interaction between pairing and time (Table 1). The probability of the visual texture being classified as hot was significantly higher after the associative learning task (.86, 95% CI = [.78, .91]) than before (.77, 95% CI = [.66, .85]; $p < .001$). As expected, under the congruent pairings, the probability was higher after the associative learning task (.97, 95% CI = [.93, .99]) than before (.75, 95% CI = [.59, .86]; $p < .001$). Furthermore, as expected, under the incongruent pairings, the probability was higher before (.79, 95% CI = [.64, .88]) than after (.54, 95% CI = [.36, .71]; $p < .001$). Importantly, after the associative learning task with pairings related to the semantic path, the congruent pairings (.97, 95% CI = [.92, .99]) led to a higher probability of the *furry* visual texture being classified as hot compared to the incongruent pairings (.55, 95% CI = [.30, .77]; $p < .001$). However, after the associative learning task with the affective-based pairings there was no difference between the congruent (.96, 95% CI = [.88, .99]) and the incongruent (.84, 95% CI = [.63, .94]; $p = .340$) pairings. As the fixed effects pseudo-R^2s of the models involving the furry visual texture revealed (Table 1), the influence of the associative learning task on the probability of the furry visual texture being classified as hot was greater for those based on the semantic path than those based on the affective one. That said, it is important to notice that the size of the fixed effects pseudo-R^2s was small, and the random effects explained most of the variability of the data. These results indicate that there was a high degree of variability at the individual level in the crossmodal associations between visual textures and temperature.

The logistic GLMM involving the *crystalline* visual texture revealed significant two-way interaction effects between mechanism and pairing and between pairing and time, as well as a significant three-way interaction effect of mechanism, pairing, and time (Table 1). As expected, under the affective mechanism, the probability of the *crystalline* visual texture being classified as cold was greater with the congruent pairings (.99, 95% CI = [.98, 1.00]) than with the incongruent ones (.97, 95% CI = [.92, .99]; p = .021). Similarly, under the semantic path, the probability that the crystalline visual texture was classified as cold was higher with the congruent pairings (.97, 95% CI = [.99, 1.00]) than with the incongruent ones (.96, 95% CI = [.90, .98]; p = .011). Furthermore, with the congruent pairings, the probability of the crystalline visual texture to be classified as cold was higher after the associative learning task (.99, 95% CI = [.98, 1.00]) than before (.99, 95% CI = [.98, .99]; p = .044). With the incongruent pairings, the probability that the *crystalline* visual texture was classified as cold was higher before the associative learning task (.99, 95% CI = [.98, .99]) compared to after (.87, 95% CI = [.79, .93]; p < .001).

To probe the three-way interaction in the initial model with the crystalline visual texture, we split the data across mechanism and ran two separate GLMMs. In terms of the affective mechanism, the results revealed a significant main effect of time and a significant interaction effect of pairing and time (Table 1). The probability of the *crystalline* visual texture being classified as cold was slightly lower after the associative learning task (.98, 95% CI = [.97, .99]) than before (.99, 95% CI = [.98, 1.00]; p = .010). However, the results revealed that under the congruent pairings, the probability was higher after the associative learning task (1.00, 95% CI = [.99, .1.00]) than before (.99, 95% CI = [.98, 1.00]; p = .016). On the other hand, under the incongruent pairing the probability was higher before the associative learning task (.99, 95% CI = [.97, 1.00]) than after (.86, 95% CI = [.94, .98]; $p < .001$). As per the semantic path, the results revealed a significant effect of the interaction between pairing and time (Table 1). Under the incongruent pairings, the probability of the *crystalline* visual texture being classified as cold was higher before the associative learning task (.99, 95% CI = [.98, 1.00]) than after (.59, 95% CI = [.76, .88]; $p < .001$). There was no significant difference in the probability before (.99, 95% CI = [.97, 1.00]) and after (.99, 95% CI = [.98, 1.00]; $p < .001$) the associative learning task with the congruent pairings. Similar to the *furry* visual texture models, the fixed factors pseudo-R^2s involving the crystalline one revealed that the effect of the pairings in the associative learning task was greater with the semantic-based pairings than the affective-based (Table 2). In this case the semantic ones were more than four and a half times larger than the affective ones. Similar to the furry visual texture, the size of the fixed effects pseudo-R^2s was small, and the random effects explained most of the variability in the data.

Reaction Times

Resulting from the identification and treatment of outliers in the reaction time data, 1,250 of the 12,000 trials (10.42%) were winsorized. Overall, the associative learning task had virtually no effect on participants' reaction times (Figure 5).

Figure 5

Raincloud Plots of RTs in Experiment 1

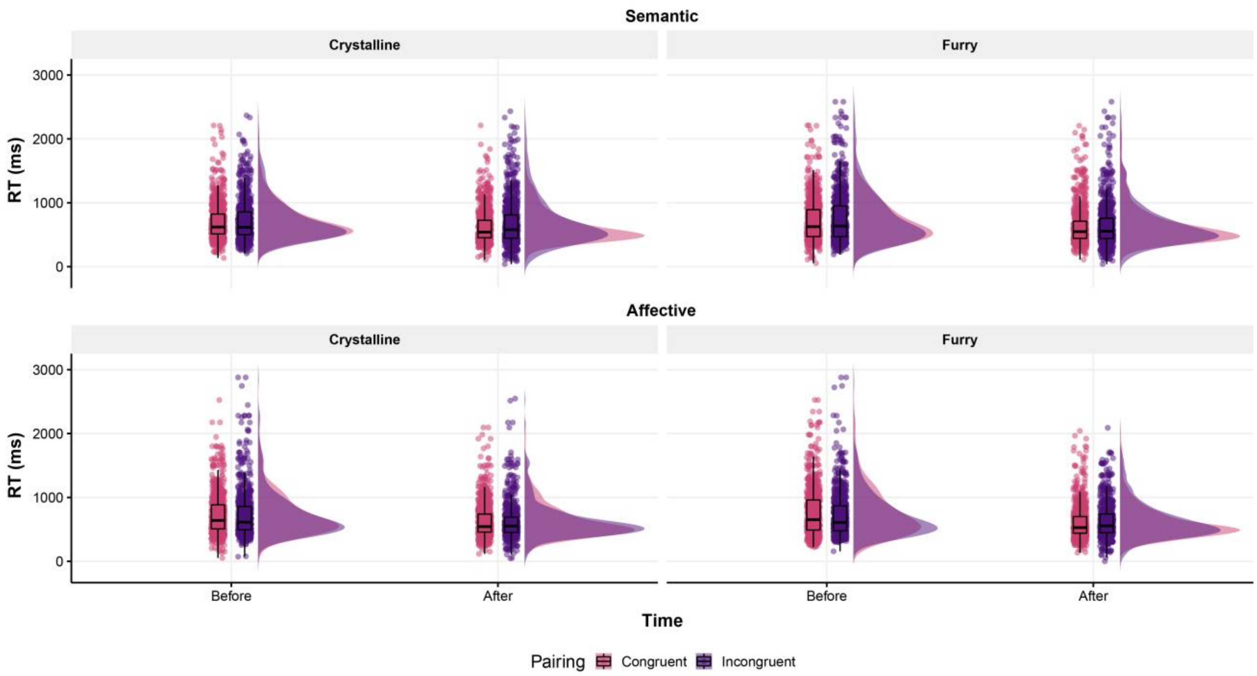

Note. The figure presents the single data points, boxplots. and distributions of the RTs per mechanism, visual texture, and pairing in Experiment 1. The timing of the speeded categorisation task, before or after the associative learning paradigm, is indicated in the x-axis.

The Gamma GLMM on reaction time under the affective-based pairings revealed a significant main effect of time, a significant two-way interaction effect of visual texture and time, and a significant three-way interaction effect of visual texture, time, and pairing. Table 3 presents the results of all the Gamma GLMMs, and Table 4 presents the results of the models fit analysis, including their corresponding pseudo-R^2s. Figure 6 presents the estimated marginal means deriving from all the Gamma GLMM models. Overall, reaction times were significantly lower after the associative learning task (643 ms, 95% CI = [623, 664]) than before (748 ms, 95% CI = [727, 770]; p < .001). Participants classified the *furry* visual texture responded more rapidly after the associative learning task (617 ms, 95% CI = [640, 662]) than before (752 ms, 95% CI = [728, 776]; $p < .001$). A similar pattern was present with the *crystalline* visual texture, as participants reacted more rapidly after the associative learning task (647 ms, 95% CI = [624, 669]) than before (745 ms, 95% CI = [721, 769]; $p < .001$). To probe the significant three-way interaction effect, we split the data by visual texture and ran two separate GLMMs. As for the *furry* visual texture, the results revealed a significant main effect of time and a significant interaction between time and pairing. Reaction times were lower after the associative learning task (637 ms, 95% CI = [613, 662]) than before (751 ms, 95% CI = [725, 778]; $p < .001$). Furthermore, under the congruent pairings, reaction times were lower after the associative learning task (631 ms, 95% CI = [597, 666]) compared to before (768 ms, 95% CI = [731, 804]; $p < .001$). Similarly, reaction times were lower after the associative learning task (643 ms, 95% CI = [608, 679]) compared to before (735 ms, 95% CI = [698, 772]; $p < .001$).

https://doi.org/10.1037/xhp0001131

Table 3

Results of the Gamma GLMM models in Experiment 1

	(A) Affective			(B) Semantic		
	Overall	Furry	Crystalline	Overall	Furry	Crystalline
	(1)	(2)	(3)	(4)	(5)	(6)
Intercept	746.34***	767.57***	743.13***	731.16***	739.02***	723.77***
	716.94 – 775.75	735.28 – 799.87	712.12 – 774.14	700.10 – 762.21	704.15 – 773.89	691.82 – 755.72
	(< .001)	(< .001)	(< .001)	(< .001)	(< .001)	(< .001)
VT_{Furry}	23.34			0.67		
	-4.32 – 51.00			-26.87 – 28.21		
	(.098)			(.962)		
$Time_{After}$	-94.76***	-136.2***	-95.96***	-86.63***	-89.08***	-87.76***
	-120.05 – -69.46	-162.32 – -110.08	-121.00 – -70.91	-112.37 – -60.89	-115.62 – -62.55	-113.05 – -62.47
	(< .001)	(< .001)	(< .001)	(< .001)	(< .001)	(< .001)
$Pairing_{Incongruent}$	-3.54	-32.41	-6.3	28.36	39.3	27.01
	-45.50 – 38.42	-78.14 – 13.32	-50.51 – 37.90	-15.18 – 71.90	-9.83 – 88.42	-17.84 – 71.86
	(.869)	(.165)	(.78)	(.202)	(.117)	(.238)
$VT_{Furry} \times Time_{After}$	-44.33**			-2.16		
	-80.20 – -8.47			-38.55 – 34.22		
	(.015)			(.907)		
$VT_{Furry} \times Pairing_{Incongruent}$	-31.97			17.56		
	-70.91 – 6.96			-21.23 – 56.35		
	(.107)			(.375)		
$Time_{After} \times Pairing_{Incongruent}$	-6	44.45**	-0.19	19.36	-10.42	20.88
	-41.96 – 29.96	7.49 – 81.42	-35.76 – 35.39	-16.88 – 55.59	-47.88 – 27.04	-14.77 – 56.53
	(.744)	(.018)	(.992)	(.295)	(.585)	(.251)
$VT_{Furry} \times Time_{After} \times Pairing_{Incongruent}$	60.1**			-31.42		
	9.21 – 110.98			-82.70 – 19.86		
	(.021)			(.23)		
Participants	149	149	149	151	151	151
Observations	5,960	2,980	2,980	6,040	3,020	3,020

Note. The table presents the results of all the Gamma GLMMs in Experiment 1. The values for each variable correspond, from top to bottom to its β estimate, 95% confidence interval, and *p*-value in parentheses. Models 1 – 3 relate to the *furry* visual texture, whereas models 4 – 6 relate to the *crystalline* visual texture. * $p < .05$, ** $p < .01$, *** $p < .001$.

Table 4

Model Fit Results of Gamma GLMMs in Experiment 1

Model		AIC	LRT			Pseudo-R^2s		
			d	X^2	*p*	R^2_{Model}	$R^2_{Fixed\ Effects}$	$R^2_{Random\ effects}$
Affective - Overall	Participant	82,332.0				.19		
	VT × Time × Pairing	82,049.0	7	297.5	<.001	.21	.02	.18
Affective - Furry	Participant	41,348.0				.18		
	Time × Pairing	41,186.0	3	168.0	<.001	.7	.03	.67
Affective - Crystalline	Participant	41,080.0				.19		
	Time × Pairing	40,961.0	3	125.5	<.001	.21	.02	.19
Semantic - Overall	Participant	83,610.0				.49		
	VT × Time × Pairing	83,408.0	7	196.6	<.001	.21	.01	.2
Semantic - Furry	Participant	42,054.0				.21		
	Time × Pairing	41,949.0	3	111.5	<.001	.22	.01	.21
Semantic - Crystalline	Participant	41,640.0				.19		
	Time × Pairing	41,560.0	3	85.87	<.001	.2	.01	.19

Note. The table presents the model fit results of all the logistic GLMMs in Experiment 1 against their corresponding null models. The null models only included participants' IDs. AIC = Akaike information criterion; LRT = Likelihood ratio test.

https://doi.org/10.1037/xhp0001131

https://doi.org/10.1037/xhp0001131

Figure 6

Estimated Marginal Means from the Gamma GLMM Models in Experiment 1

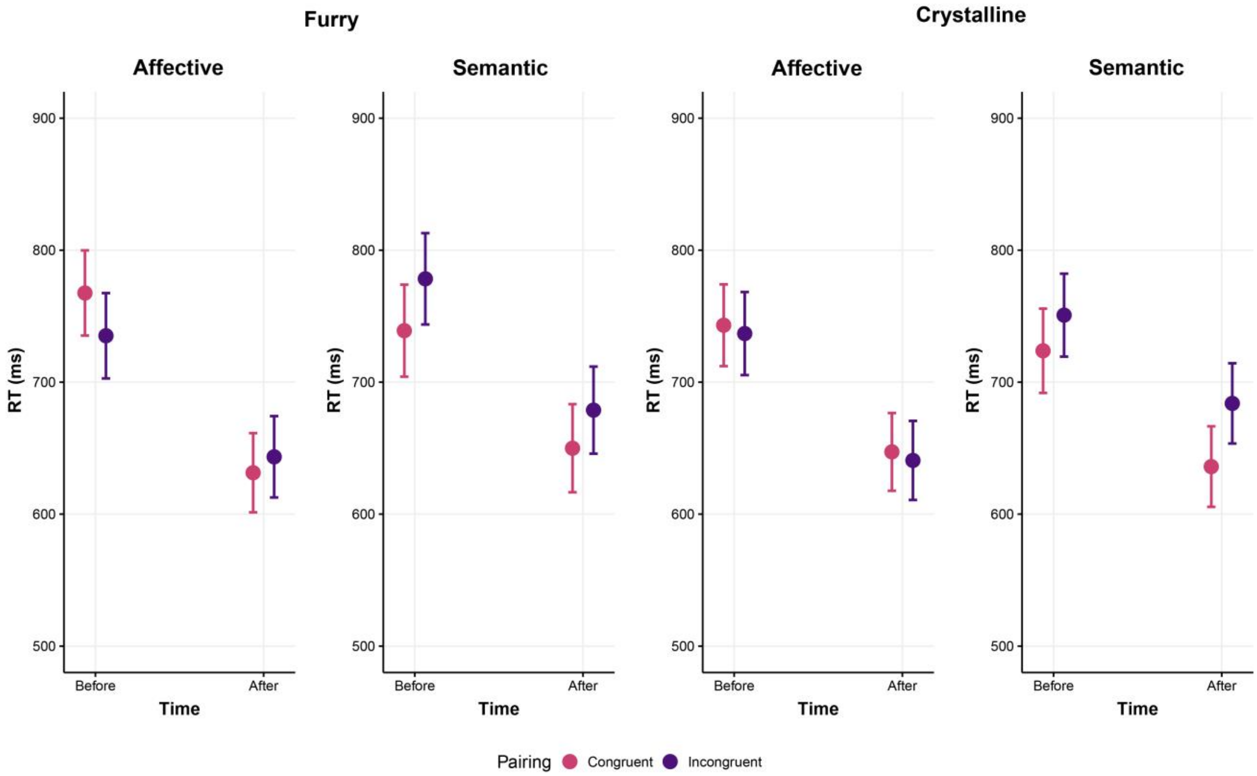

Note. The figure presents the estimated marginal means deriving from all the Gamma GLMM models in Experiment 1. The timing of the speeded categorisation task, before or after the associative learning paradigm, is indicated in the x-axis. Error bars represent the 95% CI resulting from the models.

Regarding the *crystalline* visual texture, the results revealed only a significant main effect of time. Participants responded to the categorisation task more rapidly after (644 ms, 95% CI = [620, 668]; $p < .001$) the associative learning task than before (740 ms, 95% CI = [715, 765]; $p < .001$). As per the Gamma GLMM involving the semantic-based pairings, the results revealed only a significant main effect of time (Table 3). Participants' reaction times were lower after the associative learning task (664 ms, 95% CI = [642, 686]; $p < .001$) than before (750 ms, 95% CI = [728, 772]; $p < .001$).

The fixed effects pseudo-R^2 of all the Gamma models revealed that the effects of the associative learning task involving the pairings based on the semantic path were larger than those based on the affective mechanism (Table 4). Nevertheless, the random effects pseudo-R^2s were larger than the corresponding fixed effects pseudo-R^2s, suggesting that there are relatively large individual differences in the categorisation of the visual textures as cold or hot.

In sum, the results of Experiment 1 revealed that the associative learning task increased the probability of the visual textures (i.e., *furry* and *crystalline*) being classified as either hot or cold depending on the specific affective and semantic stimuli used. Supporting H_{1A}, the congruent mappings based on the affective account led to a higher probability that the two visual textures were classified with the temperature association found by previous studies (i.e., *furry* – hot, *crystalline* – cold). In addition, the incongruent pairings reduced this probability, providing further support to H_{1A}. Furthermore, the congruent and incongruent mappings based on the semantic account had larger effects than the mappings based on the affective account, supporting H_{3A}. Even though the pairings in the associative learning task influenced the probability that the visual textures were classified in the as either cold or hot, they did not influence participants reaction time in the categorisation task. All participants reacted more rapidly after the associative learning task, but there was no difference between congruent and incongruent pairings, therefore failing to support to H_{2A} and H_{2B}. Moreover, there was no difference in the reaction times between the congruent and incongruent mappings after the associative learning, which failed to support H_{2A} and H_{2B}.

https://doi.org/10.1037/xhp0001131

Experiment 2

In Experiment 2, we extend the findings of the first experiment to visual textures without consensual associations with temperature concepts. The goal of Experiment 2 was to investigate novel crossmodal associations between these visual textures and temperature concepts can be created by establishing the mappings between these visual textures and the same affective and semantic stimuli as in Experiment 1. Investigating the creation of new associations can provide more robust evidence as to the relative strength of the studied mechanisms.

Methods

Participants

A total of 300 native English speakers from the UK (152 females, 145 males, 3 unreported), aged 18 – 40 years (M_{age} = 31.25 years, SD_{age} = 5.73) took part in the experiment.

Apparatus and Materials

For the visual textures stimuli, we selected two visual textures with no consensual associations with temperature concepts found (Barbosa Escobar et al., 2022a), which were extracted from the Describable Textures Dataset (DTD; Cimpoi et al., 2014). We selected the *stained* and the *wrinkled* visual textures. Similar to Experiment 1, we applied a pencil sketch filter to the visual textures using the IMAGETOSKETCH (https://imagetosketch.com/) website, and they were histogram equalised in Adobe Photoshop 22.1.1. The stimuli for both the affective and the semantic mappings were the same as in Experiment 1.

Design and Procedure

Experiment 2 also followed a 2 (Mechanism: affective, semantic) × 2 (Pairing: pairing 1, pairing 2) × 2 (Time: before learning, after learning) mixed design, with mechanism and pairing as between-subjects factors and time as within-subject factor. Hence, each participant was randomly assigned to one of the four possible associative learning groups derived from the interaction between mechanism and pairing. Given that we selected visual textures with no consensual temperature associations, the pairings are denoted as pairing 1 and pairing 2. Figure 7 presents all the possible mappings in the associative learning task in Experiment 2. That said, the pairings were analysed based on the temperature the stimuli paired to the visual texture was related to. Namely, as stated before, the cold-related stimuli were the sad emoji expression and the word *metal*, and the hot-related stimuli were the happy emoji expression and the word *fur*. The procedure was identical to that of Experiment 1.

Figure 7

Possible Mappings in the Associative Learning Task in Experiment 2

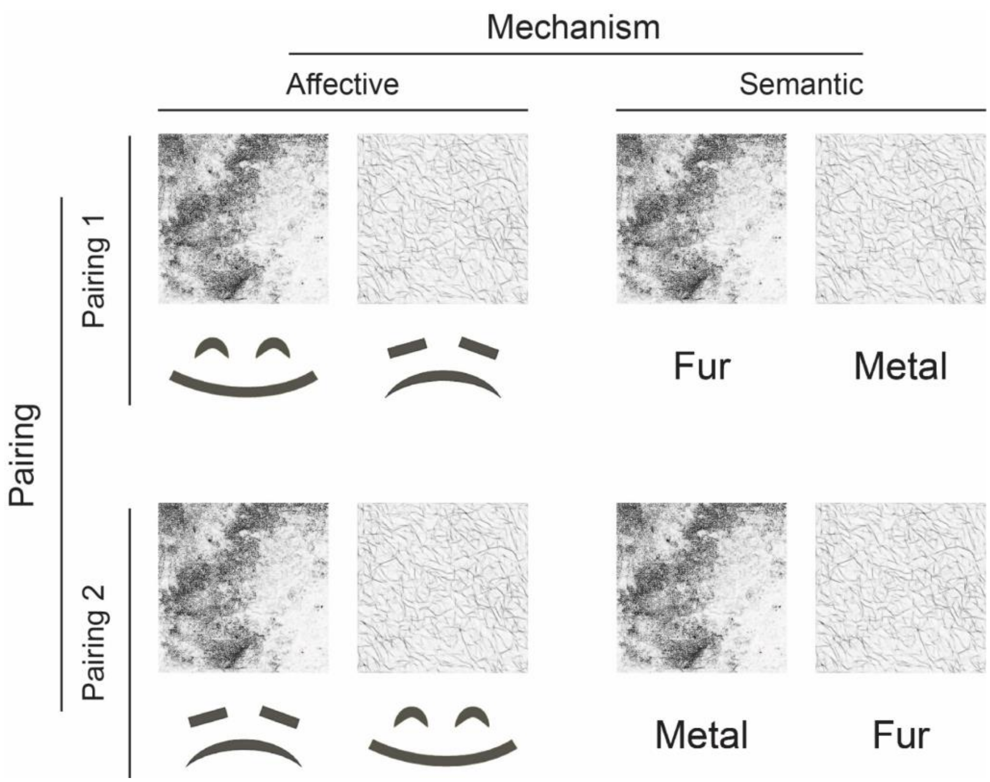

Note. The figure presents the four different mappings in Experiment 2 based on the interaction of mechanism and pairing.

Data Analysis

The data analysis was the same as in Experiment 1, except that the pairing factor was analysed as cold-related and hot-related, depending on whether the visual texture was paired with an affective or semantic stimulus related to low (sad emoji expression, the word *metal*) or high (happy emoji expression, the word *fur*) temperatures. Furthermore, to improve standardization, clarity, and ease of interpretation in the logistic GLMMs, for both visual textures, we analysed the probability that they were classified as hot.

Results

The results showed that participants obtained a high percentage of correct responses in the associative learning task (M = 98.43%, SD = 4.47%), showing that participants learned the mappings. Out of the 300 participants, 217 scored 100%. Only two participants scored less than 80% of correct responses. There were no significant differences in the percentage of correct responses between the affective and the semantic mappings, $F(1, 298) = 1.92$, $p = .167$, $\eta_p^2 = .006$; $M_{semantic}$ = 98.8%, $SD_{semantic}$ = 3.0% vs. $M_{affective}$ = 98.1%, $SD_{affective}$ = 5.9%. Participants responded faster to the semantic mappings than to the affective ones in the associative learning task, $F(1, 298) = 10.50$, $p = .001$, $\eta_p^2 = .017$; $M_{semantic}$ = 1,401 ms, $SD_{semantic}$ = 523.27 vs. $M_{affective}$ = 1,522 ms, $SD_{affective}$ = 388.89.

Categorisation Responses

The log-likelihood ratio goodness of fit tests revealed that there was a significant association between all the factors for the *stained*, $G^2(15) = 440.79$, $p < .001$, and for the *wrinkled*, $G^2(15) = 2650.9$, $p < .001$ visual textures. Figure 8 presents the mosaic plots for the categorisation responses for both visual textures. As expected, the *stained* visual texture was classified as hot as often as cold before the speeded association task. After being exposed to the hot-related affective and semantic mappings, participants classified the stained visual texture as hot more often than cold. In terms of the cold-related mappings, after being exposed to the semantic mappings, participants classified the stained visual texture as cold slightly more often than cold. However, with the affective mappings, participants classified the visual texture as hot more often than cold. Regarding the *wrinkled* visual texture, unexpectedly, participants classified it as cold much more often than hot at the beginning, possibly due to the pencil sketch filter applied to the visual texture. After the associative learning task with the hot-related pairings, both affective and semantic, participants classified the wrinkled visual texture as hot slightly more often compared to before the associative learning task. Nevertheless, the visual texture was still classified as cold more often. As per the cold-related pairings, they had virtually no effect in the categorisation of the *wrinkled* visual texture.

https://doi.org/10.1037/xhp0001131

Figure 8

Mosaic Plots of Categorisation Responses in Experiment 2

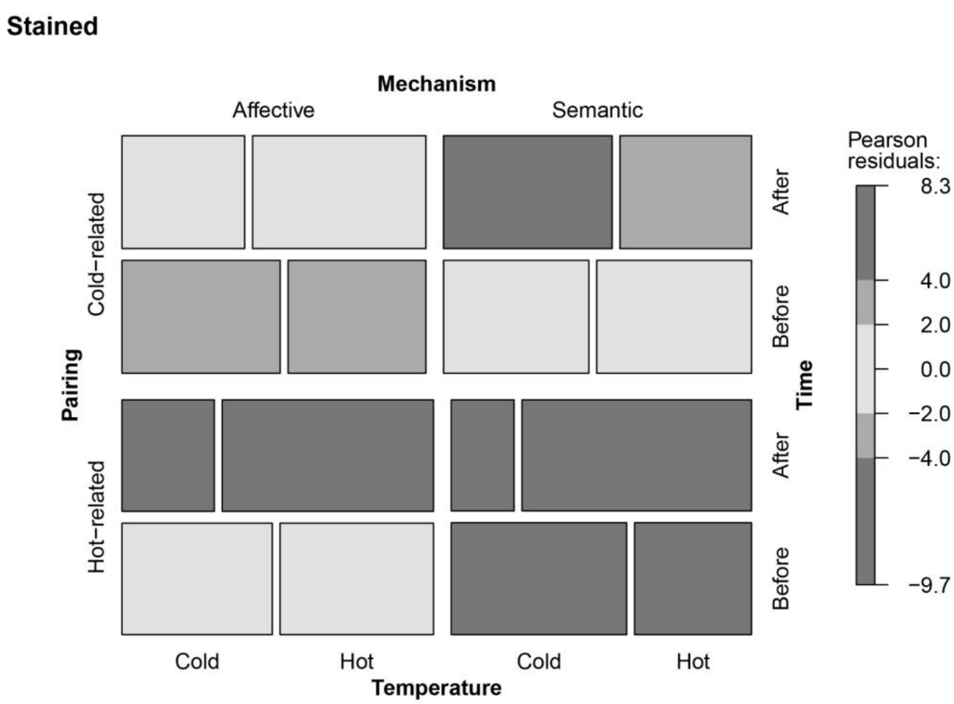

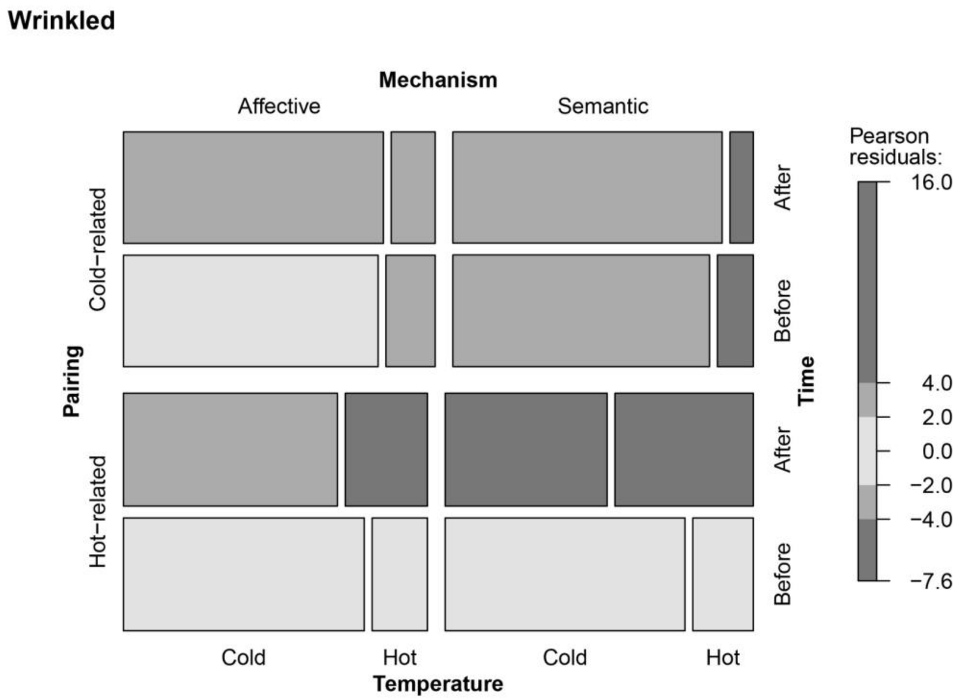

Note. The mosaic plots show the proportion in which each visual texture (*stained* in the upper panel and *wrinkled* in the lower panel) was classified as either cold or hot (indicated on the bottom side) before and after the associative learning paradigm (indicated on the left-hand side) comprising the different mechanisms (indicated on the top side) and pairings (indicated on the right-hand side).

The logistic GLMM involving the *stained* visual texture revealed a significant main effect of time, significant two-way interaction effects between mechanism and time and between pairing and time, and a significant three-way interaction effect of mechanism, pairing, and time. Table 5 presents the results of all the logistic GLMMs, and Table 6 presents the results of the models fit analysis, including their corresponding pseudo-R^2s. Figure 9 presents estimated marginal means deriving from all the logistic GLMM models. Overall, the probability of the *stained* visual texture being classified as hot was significantly higher after the associative learning task (.78, 95% CI = [.66, .86]) than before (.34, 95% CI = [.23, .48]; $p < .001$).

Furthermore, with the affective mappings, the probability of the stained visual texture being classified as hot was higher after (.80, 95% CI = [.64, .90]) than before (.35, 95% CI = [.19, .55]; $p < .001$) the associative learning task. A similar effect was found with the semantic mappings, as the probability was higher after (.34, 95% CI = [.23, .48]) than before (.75, 95% CI = [.57, .88]; $p < .001$) the associative learning task. In addition, with the hot-related pairings, the probability that the stained visual texture was classified as hot was higher after the associative learning task (.93, 95% CI = [.85, .97]) than before (.31, 95% CI = [.16, .50]; $p < .001$). With the cold-related pairings, this probability was also higher after the associative learning task (.48, 95% CI = [.29, .68]) than before (.38, 95% CI = [.21, .59]; $p = .002$).

https://doi.org/10.1037/xhp0001131

Table 5

Results of the Logistic GLMMs in Experiment 2

	(A) Stained			(B) Wrinkled		
	Overall (1)	Affective (2)	Semantic (3)	Overall (4)	Affective (5)	Semantic (6)
Intercept	0.95	0.41	0.97	0***	0***	0***
	0.35 – 2.60	0.13 – 1.25	0.38 – 2.43	0.00 – 0.01	0.00 – 0.01	0.00 – 0.01
	(.92)	(.117)	(.941)	(< .001)	(< .001)	(< .001)
$\text{Mechanism}_{\text{Affective}}$	0.43			2.15		
	0.10 – 1.81			0.27 – 17.04		
	(.25)			(.468)		
$\text{Pairing}_{\text{Hot-related}}$	0.29	1.72	0.31	9.34*	2.28	8.24
	0.07 – 1.22	0.35 – 8.34	0.08 – 1.17	1.35 – 64.74	0.31 – 16.93	1.34 – 50.63
	(.091)	(.501)	(.085)	(.024)	(.42)	(.023)
$\text{Time}_{\text{After}}$	0.45***	5.26***	0.45***	0.37***	0.69	0.37***
	0.33 – 0.63	3.49 – 7.94	0.32 – 0.62	0.22 – 0.63	0.43 – 1.11	0.22 – 0.64
	(< .001)	(< .001)	(< .001)	(< .001)	(.129)	(< .001)
$\text{Mechanism}_{\text{Affective}} \times \text{Pairing}_{\text{Hot-related}}$	6			0.23		
	0.78 – 45.91			0.02 – 3.22		
	(.085)			(.272)		
$\text{Mechanism}_{\text{Affective}} \times \text{Time}_{\text{After}}$	10.95***			1.86		
	6.50 – 18.42			0.91 – 3.80		
	(< .001)			(.088)		
$\text{Pairing}_{\text{Hot-related}} \times \text{Time}_{\text{After}}$	169.31***	2.23**	160.45***	59.5***	7.24***	57.89***
	91.74 – 312.49	1.22 – 4.05	87.74 – 293.41	29.95 – 118.23	3.69 – 14.19	29.21 – 114.74
	(< .001)	(.009)	(< .001)	(< .001)	(< .001)	(< .001)
$\text{Mechanism}_{\text{Affective}} \times \text{Pairing}_{\text{Hot-related}} \times \text{Time}_{\text{After}}$	0.01***			0.12***		
	0.01 – 0.03			0.05 – 0.31		
	(< .001)			(< .001)		
Participants	300	151	149	300	151	149
Observations	6,005	3,020	2,985	6,004	3,020	2,984

Note. The table presents the results of all the logistic GLMMs in Experiment 2. The values for each variable correspond, from top to bottom to the odds ratio, 95% confidence interval, and *p*-value in parentheses. Models 1 – 3 relate to the *stained* visual texture, whereas models 4 – 6 relate to the *wrinkled* visual texture. * $p < .05$, ** $p < .01$, *** $p < .001$.

Table 6

Model Fit Results of Logistic GLMMs in Experiment 2

Model		AIC	LRT			Pseudo-R^2s		
			d	X^2	*p*	R^2_{Model}	$R^2_{Fixed\ Effects}$	$R^2_{Random\ effects}$
Stained - Overall	Participant	3,169.0				.62		
	Mechanism × Pairing × Time	2,814.4	7	368.5	<.001	.7	.08	.62
Stained - Affective	Participant	1,416.3				.67		
	Pairing × Time	1,363.9	3	58.3	<.001	.7	.02	.68
Stained - Semantic	Participant	1,755.4				.57		
	Pairing × Time	1,451.9	3	309.5	<.001	.71	.13	.58
Wrinkled - Overall	Participant	4,661.4				.61		
	Mechanism × Pairing × Time	3,932.2	7	743.2	<.001	.72	.06	.65
Wrinkled - Affective	Participant	2,096.2				.58		
	Pairing × Time	1,868.9	3	233.2	<.001	.74	.03	.7
Wrinkled - Semantic	Participant	2,564.3				.42		
	Pairing × Time	2,062.8	3	507.4	<.001	.7	.09	.61

Note. The table presents the model fit results of all the logistic GLMMs in Experiment 2 against their corresponding null models. The null models only included participants' IDs. AIC = Akaike information criterion; LRT = Likelihood ratio test.

Figure 9

Estimated Marginal Means from the Logistic GLMM Models in Experiment 2

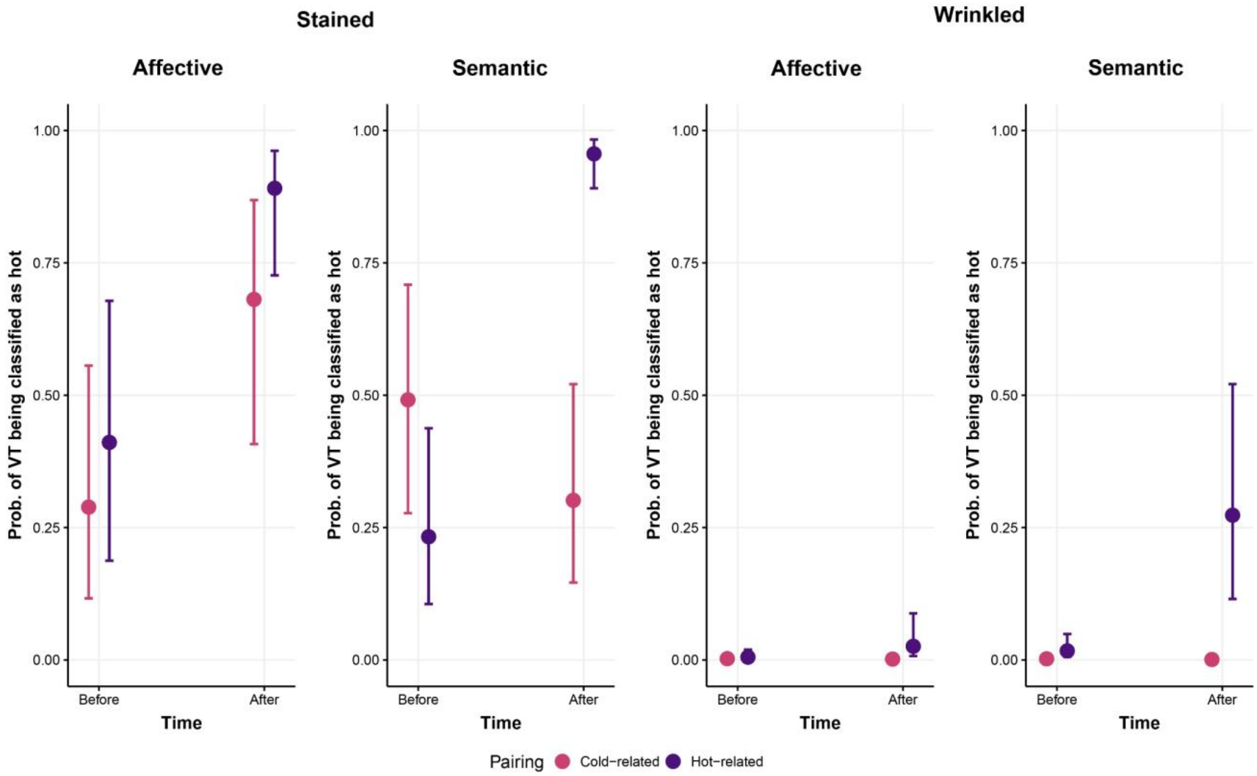

Note. The figure presents the estimated marginal means deriving from all the logistic GLMM models in Experiment 2. The y-axis represents the probability that the visual textures were classified as hot. The timing of the speeded categorisation task, before or after the associative learning paradigm, is indicated in the x-axis. Error bars represent the 95% CI resulting from the models. VT = visual texture.

To probe the three-way interaction in the first model involving the *stained* visual texture we ran two separate GLMMs splitting the data by mechanism. In terms of the affective mechanism, the results revealed a significant main effect of time and a significant two-way interaction of pairing and time (Table 5). The probability that the *stained* visual texture was

https://doi.org/10.1037/xhp0001131

classified as hot was higher after the associative learning task (.81, 95% CI = [.63, .91]; $p < .001$) compared to before (.35, 95% CI = [.18, .57]; $p < .001$). Furthermore, with the hot-related pairings, the probability of the visual texture being classified as hot was higher after (.89, 95% CI = [.69, .97]) than before (.41, 95% CI = [.16, .71]; $p < .001$) the associative learning task. Surprisingly, the cold-related pairings had a similar effect, as the probability that the stained visual texture was classified as hot was higher after the associative learning task (.68, 95% CI = [.37, .89]) than before (.29, 95% CI = [.10, .60]; $p < .001$). As per the semantic mechanism, the results revealed a significant main effect of time and a significant interaction effect of pairing and time (Table 5). The probability that the *stained* visual texture was classified as hot was higher after the associative learning task (.75, 95% CI = [.59, .87]) than before (.35, 95% CI = [.20, .54]; $p < .001$). Moreover, with the hot-related pairings, this probability was higher after (.96, 95% CI = [.88, .99]) than before (.23, 95% CI = [.09, .47]; $p < .001$) the associative learning task. On the contrary, with cold-related pairings, the probability that the stained visual texture would be classified as hot was lower after the associative learning task (.30, 95% CI = [.13, .55]) than before (.49, 95% CI = [.25, .74]; $p < .001$).

The logistic GLMM involving the wrinkled visual texture revealed main effects of pairing and time, as well as a significant two-way interaction effect of pairing and time, and a significant three-way interaction effect of mechanism, pairing, and time (Table 5). The probability of the wrinkled visual texture being classified as hot was higher with the hot-related pairings (.033, 95% CI = [.014, .081]) in the associative learning task than with the cold-related ones (.002, 95% CI = [.001, .006]; $p < .001$). In addition, the probability that the visual texture was classified as hot was higher after the associative learning task (.012, 95% CI = [.005, .025]) than before (.005, 95% CI = [.002, .011]; $p < .001$). Furthermore, with the hot-related pairings, the probability that the wrinkled visual texture was classified as hot was higher after the associative learning task (.101, 95% CI = [.042, .222]) than before (.011, 95% CI = [.004, .027]; $p < .001$).

As with the *stained* visual texture, to probe the three-way interaction in the first model involving the *wrinkled* visual texture we ran two separate GLMMs splitting the data by mechanism. In terms of the affective mechanism, the results revealed a significant two-way interaction effect of pairing and time (Table 5). With the hot-related pairings, the probability that the wrinkled visual texture was classified as hot was higher after (.026, 95% CI = [.006, .104]) than before (.005, 95% CI = [.001, .023]; $p < .001$) the associative learning task. However, with the cold-related pairings, there was no significant difference in the probability of the wrinkled visual texture being classified as hot after (.001, 95% CI = [< .001, .009]) compared to before (.002, 95% CI = [< .001, .123]; $p = .129$) the associative learning task. As per the semantic path, the results revealed significant main effects of pairing and time and a significant two-way interaction effect of pairing and time. The probability that the wrinkled visual texture was classified as hot was higher with the hot-related pairings (.075, 95% CI = [.024, .212]; $p < .001$) than with the cold-related ones (.001, 95% CI = [< .001, .007]; $p < .001$). Moreover, the probability that the visual texture was classified as hot was higher after the associative learning task (.017, 95% CI = [.006, .047]) than before (.006, 95% CI = [.002, .017]; $p < .001$). Furthermore, under the hot-related pairings, the probability that the wrinkled visual texture was classified as hot was higher after the associative learning task (.273, 95% CI = [.100, .599]) than before (.017, 95% CI = [.005, .057]; $p < .001$). However, this probability was lower after the associative learning task (< .001, 95% CI = [< .001, .004]) than before (.002, 95% CI = [< .001, .011]; $p < .001$) with the cold-related pairings.

https://doi.org/10.1037/xhp0001131

Reaction Times

Resulting from the identification and treatment of outliers in the reaction time data, 1,163 of the 12,000 trials (9.69%) were winsorized. Overall, similar to Experiment 1, the associative learning task had virtually no effect on participants' reaction times (Figure 10). The Gamma GLMM on reaction times with the affective-based pairings revealed only a significant main effect of time. Table 7 presents the results of all the logistic GLMMs, and Table 8 presents the results of the models fit analysis, including their corresponding pseudo-R^2s. Figure 11 presents the estimated marginal means deriving from all the logistic GLMM models Reaction times were significantly lower after the associative learning task (606 ms, 95% CI = [584, 628]) than before (752 ms, 95% CI = [729, 776]; $p < .001$). Similarly, the GLMM on the reaction times with the semantic-based pairings revealed that reaction times were significantly lower after the associative learning task (659 ms, 95% CI = [636, 682]) than before (772 ms, 95% CI = [748, 795]; $p < .001$).

Figure 10

Raincloud Plots of RTs in Experiment 2

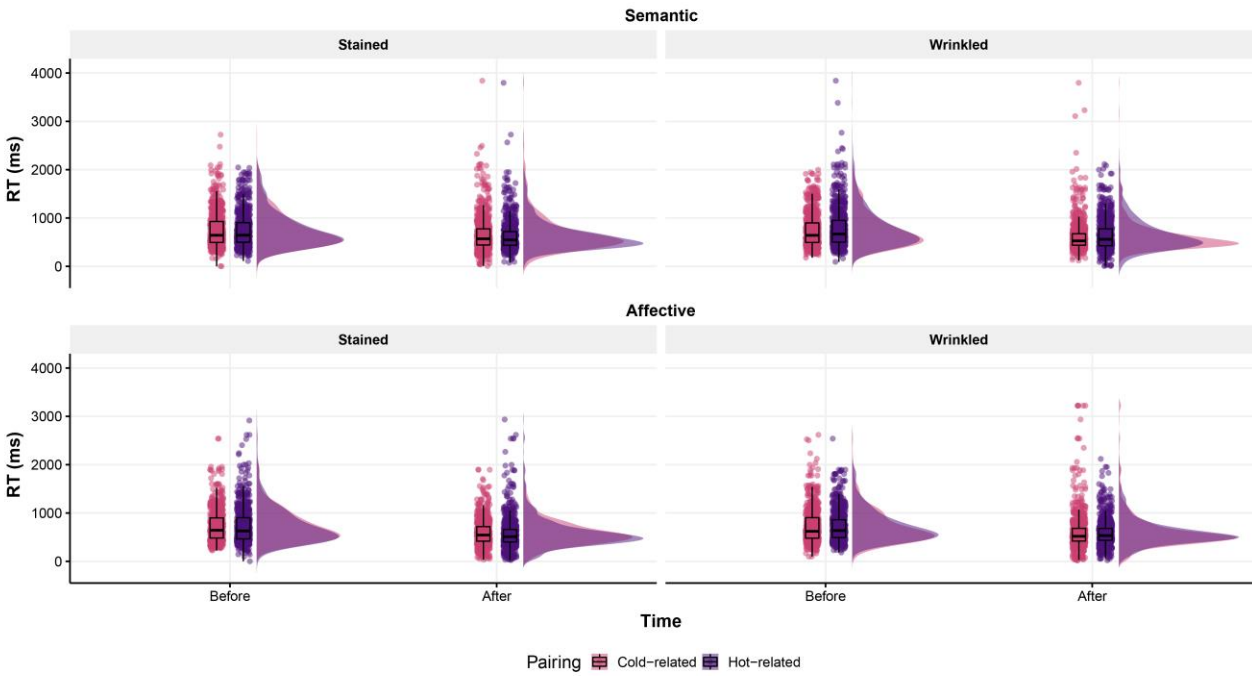

Note. The figure presents the single data points, boxplots. and distributions of the reaction times in per mechanism, visual texture, and pairing in Experiment 2. The timing of the speeded categorisation task, before or after the associative learning paradigm, is indicated in the x-axis.

https://doi.org/10.1037/xhp0001131

https://doi.org/10.1037/xhp0001131

Table 7

Results of the Gamma GLMMs in Experiment 2

	(A) Affective			(B) Semantic		
	Overall (1)	Stained (2)	Wrinkled (3)	Overall (4)	Stained (5)	Wrinkled (6)
Intercept	740.66***	744.57***	765***	780.7***	779.18***	748.3***
	708.41 – 772.90	710.79 – 778.35	731.01 – 798.99	748.20 – 813.21	744.07 – 814.29	713.64 – 782.95
	(< .001)	(< .001)	(< .001)	(< .001)	(< .001)	(< .001)
$VT_{Wrinkled}$	19.92			-28.51		
	-25.49 – 65.33			-74.70 – 17.68		
	(.39)			(.226)		
$Time_{After}$	-132.5***	-138.09***	-161.96***	-108.28***	-107.77***	-113.75***
	-159.13 – -105.87	-164.78 – -111.40	-187.26 – -136.65	-135.42 – -81.14	-135.38 – -80.17	-141.31 – -86.18
	(< .001)	(< .001)	(< .001)	(< .001)	(< .001)	(< .001)
$Pairing_{Hot\text{-}related}$	24.39	15.09	-22.27	-27.29	-23.94	47.23
	-21.08 – 69.87	-32.54 – 62.71	-70.51 – 25.96	-73.49 – 18.91	-73.86 – 25.98	-1.81 – 96.27
	(.293)	(.535)	(.365)	(.247)	(.347)	(.059)
$VT_{Wrinkled} \times Time_{After}$	-18.62			-2.02		
	-55.64 – 18.41			-40.37 – 36.34		
	(.324)			(.918)		
$VT_{Wrinkled} \times Pairing_{Hot\text{-}related}$	-41.59			75.37		
	-122.50 – 39.31			-7.21 – 157.95		
	(.314)			(.074)		
$Time_{After} \times Pairing_{Hot\text{-}related}$	-33.79	-32.01	25.99	8.49	7.7	-19.33
	-70.75 – 3.17	-69.08 – 5.06	-10.69 – 62.67	-30.05 – 47.04	-31.48 – 46.87	-58.63 – 19.96
	(.073)	(.091)	(.165)	(.666)	(.7)	(.335)
$VT_{Wrinkled} \times Time_{After} \times Pairing_{Hot\text{-}related}$	49.87			-30.82		
	-2.53 – 102.28			-85.42 – 23.78		
	(.062)			(.268)		
Participants	151	151	151	149	149	149
Observations	6,040	3,020	3,020	5,969	2,985	2,984

Note. The table presents the results of all the Gamma GLMMs in Experiment 2. The values for each variable correspond, from top to bottom to its β estimate, 95% confidence interval, and *p*-value in parentheses. Models 1 – 3 relate to the *stained* visual texture, whereas models 4 – 6 relate to the *wrinkled* visual texture. * $p < .05$, ** $p < .01$, *** $p < .001$.

Table 8

Model Fit Results of Gamma GLMMs in Experiment 2

Model		AIC	LRT			Pseudo-R^2s		
			d	X^2	*p*	R^2_{Model}	$R^2_{Fixed\ Effects}$	$R^2_{Random\ effects}$
Affective - Overall	Participant	84,096.0				.18		
	VT × Time × Pairing	83,601.0	7	509.4	<.001	.2	.02	.18
Affective - Stained	Participant	42,154.0				.19		
	Time × Pairing	41,881.0	3	278.8	<.001	.21	.03	.19
Affective - Wrinkled	Participant	42,053.0				.17		
	Time × Pairing	41,792.0	3	267.3	<.001	.19	.01	.17
Semantic - Overall	Participant	83,460.0				.18		
	VT × Time × Pairing	83,186.0	7	288.2	<.001	.19	.02	.18
Semantic - Stained	Participant	41,828.0				.18		
	Time × Pairing	41,713.0	3	120.1	<.001	.18	.01	.17
Semantic - Wrinkled	Participant	41,801.0				.16		
	Time × Pairing	41,638.0	3	168.9	<.001	.18	.02	.16

Note. The table presents the model fit results of all the Gamma GLMMs in Experiment 2 against their corresponding null models. The null models only included participants' IDs. AIC = Akaike information criterion; LRT = Likelihood ratio test.

Figure 11

Estimated Marginal Means from the Gamma GLMM Models in Experiment 2

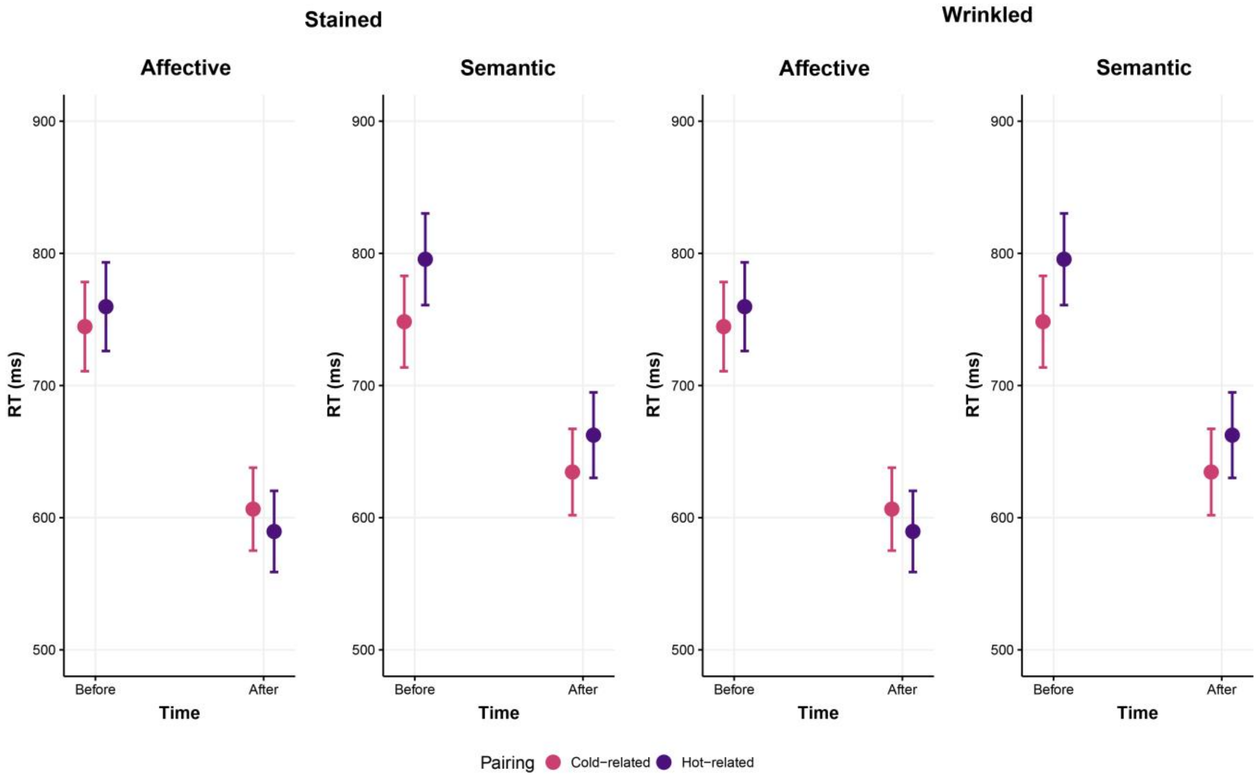

Note. The figure presents the estimated marginal means deriving from all the Gamma GLMM models in Experiment 2. The timing of the speeded categorisation task, before or after the associative learning paradigm, is indicated in the x-axis. Error bars represent the 95% CI resulting from the models.

In sum, the results of Experiment 2 revealed that an associative learning task with either affective and semantic mappings related to low- and high-temperature concepts increased the probability that the visual texture without clear consensual associations to temperature concepts (i.e., *stained*) was classified as hot or cold as hypothesised. Similar effects were found with the *wrinkled* visual texture, although this visual texture had consensual associations with low temperature. The possibility that either of the visual textures was classified as hot significantly increased when they were paired with affective and semantic content related to high temperatures, whereas the possibility that either visual texture was classified as cold significantly increased when they were paired with affective or semantic content related to low temperatures. Thus, these results provide support to H_{4A} and H_{4B}. However, there was no difference in participants' reaction times to the categorisation task whether the visual textures were paired to the affective or semantic content either related to low temperatures or high temperatures.

General Discussion

In the present study, two online experiments were conducted using an associative learning paradigm to investigate whether crossmodal associations between visual textures and temperature concepts could be created from scratch by learning mappings related to an affective mechanism or a semantic path (i.e., related to a single common source identity). In addition, the experiments investigated the relative influence of an affective mechanism and a semantic path on the existence of these associations. In Experiment 1, these effects were examined using visual textures with consensual temperature concepts associations (*crystalline* – low temperatures; *furry* – high temperatures), and in Experiment 2, visual textures with no such consensual associations (*stained*; *wrinkled*) were used. Our results demonstrated that both the affective mechanism and the semantic path can induce crossmodal associations between visual textures and temperature concepts, so these accounts are not mutually exclusive, as suggested by Spence (2011, 2020c), although the semantic path had a relatively higher strength. These results hold true based on the operationalization of the variables used here. Nevertheless, future studies may conceptually replicate and extend our results measuring the strength of the associations differently. Furthermore, the results presented here open further questions for future research. For instance, what determines the relative weight among different mechanisms in given a crossmodal

https://doi.org/10.1037/xhp0001131

associations, and are there other explanations behind the formation of crossmodal correspondences?

The results of Experiment 1 revealed that the congruent learning task increased the probability that the visual textures were classified with the corresponding hypothesised temperature concept (*crystalline* – cold; *furry* – hot) as found in a previous study on crossmodal associations between visual textures and temperature (Barbosa Escobar et al., 2022a). On the other hand, the learning task with incongruent combinations reduced such probabilities. These results highlight the plasticity associated with the formation of crossmodal associations and indicate that the incongruent pairings undid previous beliefs. Notably, overall, the semantic combinations exerted a larger influence on the categorisation results than the affective ones. The results of Experiment 2 revealed that the affective and semantic strategies significantly influenced the explicit temperature categorisation of the *stained* visual texture as hot (after the mappings related to high temperatures) and cold (after the mappings related to low temperatures). Moreover, the effect of the semantically based pairings on the categorisation responses was larger. In addition, considering the *stained* visual texture, which initially did not present consensual associations with temperature, it was easier to induce associations with hot than with cold. It is important to note that contrary to our expectations, participants strongly associated the *wrinkled* visual texture with cold at the outset, which became a boundary condition for the mappings related to low temperatures. However, the associations could be undone after the associative learning task with mappings related to high temperatures. In this case, participants' previously held associations were more easily reversed after undergoing an associative learning task with semantic mappings than with affective ones. It is worth noting that in the present study, we used low-arousal stimuli, whereas in everyday life, more intense stimuli

https://doi.org/10.1037/xhp0001131

https://doi.org/10.1037/xhp0001131

tend to form stronger associations. Considering this difference in arousal, affective stimuli that are both positively valenced and high in arousal could potentially lead to stronger effects than those found here. However, this would not be the case with negative stimuli and low temperatures, as, negative-valenced, high arousal stimuli are associated with high temperatures.

Even though the associative learning task influenced the explicit categorisation responses in Experiment 1, the congruent combinations, compared to the incongruent ones, did not influence participants' reaction time. One potential explanation is that individuals may need some level of strategizing to categorise the visual textures under both types of mappings, which may have eliminated any effect on categorisation speed. Similar to Experiment 1, the associative learning tasks in Experiment 2 did not affect participants' reaction time in the cold- vs. hot-related mappings. While reaction times in the speeded categorisation tasks were lower after the associative learning than before, this was the case for all conditions in both experiments. This could have been caused by a practice effect. Altogether, our findings indicate that relative to the affective account, the semantic path has more weight in forming these associations.

Results regarding the influence of the affective learning on texture-temperature associations were consistent with the findings of Barbosa Escobar et al. (2022a). The latter authors showed that visual textures associated with high-temperature concepts tend to be positively valenced. On the other hand, visual textures associated with low-temperature concepts tend to be negatively valenced. It is possible that furry visual textures and high (but not extreme) temperature concepts trigger similar affective reactions, as they can both generate positive feelings and sensations. The positive affect from furry visual textures may stem from their perceived softness. As previous research has found, softness is a critical factor in the affective responses to materials, especially in clothing, where higher levels of softness are associated with more positive affect (Etzi et al., 2014; Kergoat et al., 2012; Spence, 2020b; Teli, 2015). Furthermore, as Kergoat et al. (2012) found, softness is related to comfort and care, which are concepts with which warm temperatures are also associated. These latter connections may derive from the warmth and comfort provided by mothers and caregivers to their offspring after birth (Zhang & Risen, 2014) or by the warmth perceived when being physically close to loved ones (Ijzerman et al., 2015).

Furthermore, related to the semantic path, it is possible that the associations originate from semantic knowledge about a source object (or source object-based mappings). One of the best examples of these types of mappings can be observed in associations between colours and odours. Previous literature suggests that colour-odour associations occur because individuals picture the source object of the odour and then match the odour with the colour of the source (see Spence 2020a, for a review). As Kaeppler (2018) found, there is a positive relationship between consistency of colour-odour and individuals' ability to determine the odour's source. Here, the visual textures may have brought specific objects or materials to mind. Hence, the associations may have been formed based on individuals' knowledge of said materials. For instance, the *furry* visual texture may have evoked a furry animal, which itself is warm, or a furry coat, which is used to keep one's body warm. As Di Cicco et al. (2021) found in a study of perceptual material signatures in paintings from the 17th century, velvet was perceived to be furrier, softer, and warmer than satin when participants evaluated the whole painting. In addition, the *crystalline* visual texture could have evoked ice crystals, stones, or slivers/fragments of metal, which are cold to the touch.

One of the key aims of the present study was to investigate the influence of affective versus semantic learning mechanisms in the formation of crossmodal associations between visual

https://doi.org/10.1037/xhp0001131

textures and temperature. As evidenced by the difference in the GLMMs' odds ratios and pseudo-R^2s between the two mechanisms, the results seem to indicate a greater influence of the semantic path relative to an affective account. Here, it is important to note that, overall, the effect of the fixed effects pseudo-R^2s was small. Nevertheless, the GLMMs are modelling, in a fine-grained fashion, the probability that a given visual texture is classified with a specific temperature concept, which may, to some extent, decrease the overall size of the fixed effects pseudo-R^2s. In addition, it is possible that with complex, and sometimes, ambiguous stimuli, such as visual textures, individual differences in crossmodal associations are relatively large. Higher complexity and ambiguity may render people's interpretation of stimuli and the meaning extracted from them more susceptible to their individual idiosyncrasies, such as personality and past experiences. For example, as Partos et al. (2016) found, people with higher tendency to experience perceptual aberrations, magical thinking, and hallucinations are more prone to find complex meaning in images consisting of random visual noise than people with lower tendencies in these aspects. In the present study, the extent to which it is associated with a temperature concept could have been influenced by each individual's interpretation of the visual texture.

The individual differences in the crossmodal associations studied in the present study were captured by the random effects pseudo-R^2s in the different GLMMs. Given the scarcity of research explicitly studying the origin of crossmodal associations and even more so using a similar experimental and analytical approach, it is difficult to benchmark how big or small the influence of the fixed and random effects should be. Having this in mind, the present results seem to suggest that, compared to the affective account, the semantic path makes it easier to pick up associations with temperature concepts. For instance, in Experiment 1, the incongruent semantic mappings more easily undid individuals' previous associations than the incongruent

https://doi.org/10.1037/xhp0001131

affective mappings. The semantic path may be picking up on statistical regularities and correlations in the environment tied to specific entities or meaning (Parise & Spence, 2013; Spence, 2011). These associations may originate from people internalising that different (visual and tactile) textures generally have specific material properties that make them be perceived at certain temperatures when touched (Barenholtz et al., 2014; Shams & Seitz, 2008). In particular, the statistical regularities being picked up may be based on the thermal effusivity of materials, which refers to a material's ability to exchange thermal energy with its surrounding (Blaine, 2018) and is strongly correlated with the physical, thermal perception of materials (Wongsriruksa et al., 2012). Materials with low thermal effusivity feel warm to the touch, which also end up shaping the language used to describe objects and experiences (Cuskley & Kirby, 2013; Parise & Spence, 2013; Spence, 2011). Therefore, given that the semantic path may be related to the statistical regularities experienced throughout life, its influence on the formation of associations is stronger than the affective account. On the other hand, the affective account relates to more abstract concepts, which may present large differences across individuals in terms of their affective associations with specific materials.

The most relevant point in Experiment 2 is that the crossmodal associations between the visual texture with no consensual temperature associations were not created by explicitly training participants to learn temperature associations. Instead, they were created by mapping the visual texture to content related to the hypothesised affective and semantic paths behind the crossmodal associations studied here. In other words, correlations between visual textures and either affective or semantic stimuli were presented, which induced participants to establish novel crossmodal associations between visual textures and temperature concepts. These results add robustness to our hypothesis that the affective and semantic accounts are, in a non-mutually exclusive way, driving crossmodal associations between visual textures and temperature concepts. Furthermore, these results support previous research showing that crossmodal associations are plastic and do not become crystallised with age (Parise, 2016). This stands in contrast to synaesthetic mappings (i.e., inducer–concurrent mappings), which seem to be stable across individuals' adult lifetime (Deroy & Spence, 2013), although previous studies have found that some synesthetic mappings may come from statistical regularities experienced early in life, such as with the letter colours in refrigerator magnets (Beeli et al., 2007; Deroy & Spence, 2013; Smilek et al., 2007; Witthoft & Winawer, 2006). Moreover, the results of Experiment 2 provided further evidence that both the affective mechanism and the semantic path are non-mutually exclusive explanations behind crossmodal associations between visual textures and temperature concepts.

In addition, the results of both experiments revealed that there is a relatively high degree of variability across individuals in the crossmodal associations studied here. As evidenced by the higher pseudo-R^2s of the random effects compared to the pseudo-R^2s of the fixed effects across mechanisms and visual textures, the variance in the categorisation responses and reaction times was mainly explained by individual variability.

Limitations and Future Directions

It is worth noting several limitations of the present studies. First, only one image per visual texture category was used. In addition, one stimulus for each affective and semantic content category related to low and high temperatures was used. The associations could vary depending on the specific image from the given visual texture categories. Other affective and semantic stimuli related to low and high temperatures could have different levels of effect. Furthermore, specific features of the visual textures or the affective and semantic stimuli may have influenced the results. For example, the angularity of the visual textures may have influenced the associations, as high levels of angularity, such as the straight lines and sharp edges found in the crystalline visual texture, may potentially be associated with low temperatures given their shared negative valence. However, given that we used complex stimuli, this effect is hard to disentangle. Future research investigating associations between angularity and temperature using simple stimuli (e.g., a single line) could reveal interesting results.

An important limitation in our study relates to the use of emojis as affective stimuli. Previous research has shown that emojis may have both semantic and affective associations, and the meaning of emojis varies depending on the context and media platform (e.g., iOS, Android, Twitter, Facebook) in which they are used (Bai et al., 2019; Jaeger et al., 2019). It is worth noting that this research has almost exclusively used emojis found in everyday life via different platforms. As per the relationship between the emotional and semantic meaning of emojis, in a cross cultural study with US and Chinese participants, Jaeger et al. (2021) found that the semantic meaning of emojis is attributed by different levels of intensity of associations to different emotions. Emojis are an effective tool to convey emotional meaning (Novak et al., 2015), and those that are explicitly design to convey specific emotions, do it better than other means (e.g., human facial expressions; Cherbonnier & Michinov, 2021). Here, we used the facial expressions (i.e., only eyebrows and smiles) of two emojis from the EmojiGrid (Toet et al., 2018), which were explicitly developed to convey specific values of the valence and arousal dimensions of affect. Furthermore, they are not part of the official Unicode emoji and are not found people’s everyday life in any of the digital communication platforms (e.g., iOS, Android, Facebook). Thus, the emoji facial expressions used here are less likely to have the semantic associations attributed to the emojis people use every day (e.g., 😊, 😞). However, it should be noted that the emoji facial expressions here may still carry semantic associations.

Furthermore, another limitation is that the semantic stimuli were the words *fur* and *metal*, while one of the visual textures was fur. In the congruent condition, the fur visual texture was mapped to the word fur, whereas the crystalline visual texture was mapped with metal. The high degree of congruency in the former case could have affected the learning process for the two visual textures differently. Nevertheless, the pseudo-R^2s effects of the overall model and the fixed effects of the semantic mappings were higher for the crystalline than for the furry visual texture. An aspect to consider is that the learning rate of semantic compared to affective information may be different, as semantic categorization tends to occur before affective categorization and both depend on visual awareness (Lähteenmäki & Nummenmaa, 2015). The mappings involving the semantic stimuli, which may presumably be easier to learn, could have led to a larger effect of the semantic mappings than the affective ones on the categorisation responses.

Moreover, our sample was limited to English native speakers based in the UK. It is not possible to generalise these findings to individuals in other countries or whose native language is not English, as there may be non-negligible differences in the environmental statistics they have been exposed to, as well as their semantic networks and language their encoded into. On a similar note, participants were between 18 and 40 years old. Therefore, there may be differences in these associations that are driven by age that we did not detect. Regarding our experimental paradigm in the associative learning task, we created two pairs of mappings, one for each of the two visual textures. It cannot be discarded that the speeded categorisation task responses were biased by only having two mappings.

https://doi.org/10.1037/xhp0001131

Future research can build on the present study to further the understanding of the underlying mechanisms of these crossmodal associations. For instance, future studies may use a larger number of visual textures, as well as larger number of affective and semantic stimuli in the learning process. In addition, given the prominent role of softness in the affective responses to materials (Etzi et al., 2014; Kergoat et al., 2012; Spence, 2020b; Teli, 2015), it would be interesting to examine whether higher perceived softness leads to a stronger association with high temperatures. A similar method could be applied to examine varying levels of valence. Furthermore, given the potential role of experience and language in statistical and semantic associations, examining different group levels, including children, would yield interesting results.

Conclusion

Taken together, our findings show that crossmodal associations can be strengthened, weakened, and created via associative learning mappings related to an affective mechanism and a semantic path, and not only by explicitly mapping the specific dimensions/stimuli involved in the crossmodal associations as previous literature has shown. Furthermore, our results seem to suggest that relative to an affective account, a semantic path leads to the formation of stronger crossmodal associations between visual textures and temperature concepts. This semantic account may be building on the identity of a specific object and consequently on a statistical account through the internalisation of environmental statistics. Thus, these mechanisms are interrelated and may overlap. In addition, the semantic path may also establish affective associations given the repeated affective reactions triggered by objects, textures, and material properties. As Spence (2020d) suggested, different accounts (i.e., statistical, structural, lexical, affective) of crossmodal correspondences are not mutually exclusive, but instead they may all

https://doi.org/10.1037/xhp0001131

have some explanatory power for the existence of these associations (Spence, 2011, 2020c). Furthermore, the results presented here suggest that crossmodal associations between visual textures and temperature present a relatively high variability across individuals. Notably, we demonstrated that the associations between ambiguous visual textures and temperature concepts could be modulated by learning. Our work adds to the literature on crossmodal correspondences, and most importantly, it empirically investigates, using a new paradigm, the relative role of two potential mechanisms underlying a novel set of crossmodal associations, which only a limited number of studies to date have done. Although it is difficult to disentangle the mechanisms behind crossmodal associations, the present study deepens the understanding of how individuals establish crossmodal associations between visual textures and temperature. Moreover, this research serves as a platform for future more exhaustive studies on how different types of crossmodal associations are formed.

References

American Psychological Association. (n.d.). Visual texture. In *APA dictionary of psychology*. Retrieved August 1, 2022, from https://dictionary.apa.org/visual-texture

Bai, Q., Dan, Q., Mu, Z., & Yang, M. (2019). A systematic review of emoji: Current research and future perspectives. *Frontiers in Psychology*, *10*, 2221. https://doi.org/10.3389/fpsyg.2019.02221

Barbosa Escobar, F., Velasco, C., Byrne, D. V., & Wang, Q. J. (2022a). Crossmodal associations between visual textures and temperature concepts. *Quarterly Journal of Experimental Psychology*. https://doi.org/10.1177/17470218221096452

Barbosa Escobar, F., Velasco, C., Byrne, D. V., & Wang, Q. J. (2022b). The influence of emotional cues and anthropomorphism on product temperature expectations. *PsyArXiv*. https://doi.org/10.31234/osf.io/v6p2e

Barbosa Escobar, F., Velasco, C., Motoki, K., Byrne, D. V., & Wang, Q. J. (2021). The temperature of emotions. *PLOS ONE*, *16*(6), e0252408. https://doi.org/10.1371/journal.pone.0252408

Barenholtz, E., Lewkowicz, D. J., Davidson, M., & Mavica, L. (2014). Categorical congruence facilitates multisensory associative learning. *Psychonomic Bulletin and Review*, *21*(5), 1346–1352. https://doi.org/10.3758/s13423-014-0612-7

Bates, D., Mächler, M., Bolker, B. M., & Walker, S. C. (2015). Fitting linear mixed-effects models using lme4. *Journal of Statistical Software*, *67*(1), 1–48. https://doi.org/10.18637/jss.v067.i01

Beeli, G., Esslen, M., & Jäncke, L. (2007). Frequency correlates in grapheme-color synaesthesia. *Psychological Science*, *18*(9), 788–792. https://doi.org/10.1111/j.1467-9280.2007.01980.x

Bergmann Tiest, W. M., & Kappers, A. M. L. (2009). Tactile perception of thermal diffusivity. *Attention, Perception, & Psychophysics*, *71*(3), 481–489. https://doi.org/10.3758/APP.71.3.481

Blaine, R. L. (2018). In search of thermal effusivity reference materials. *Journal of Thermal Analysis and Calorimetry*, *132*(2), 1419–1422. https://doi.org/10.1007/s10973-018-7020-6

Brunel, L., Carvalho, P. F., & Goldstone, R. L. (2015). It does belong together: Cross-modal correspondences influence cross-modal integration during perceptual learning. *Frontiers in Psychology*, *6*. https://doi.org/10.3389/fpsyg.2015.00358

Chen, Y.-C., & Spence, C. (2010). When hearing the bark helps to identify the dog: Semantically-congruent sounds modulate the identification of masked pictures. *Cognition*, *114*(3), 389–404. https://doi.org/10.1016/j.cognition.2009.10.012

Chen, Y.-C., & Spence, C. (2017). Assessing the role of the “unity assumption” on multisensory integration: A review. *Frontiers in Psychology*, *8*, 445. https://doi.org/10.3389/fpsyg.2017.00445

Cherbonnier, A., & Michinov, N. (2021). The recognition of emotions beyond facial expressions: Comparing emoticons specifically designed to convey basic emotions with other modes of expression. *Computers in Human Behavior*, *118*, 106689. https://doi.org/10/fqq5

Cimpoi, M., Maji, S., Kokkinos, I., Mohamed, S., & Vedaldi, A. (2014). Describing textures in the wild. *Proceedings of the IEEE Computer Society Conference on Computer Vision and Pattern Recognition*, 3606–3613. https://doi.org/10.1109/CVPR.2014.461

Cottrill, A. L., Liu, A. T., Kunai, Y., Koman, V. B., Kaplan, A., Mahajan, S. G., Liu, P., Toland, A. R., & Strano, M. S. (2018). Ultra-high thermal effusivity materials for resonant ambient thermal energy harvesting. *Nature Communications*, *9*(1), 1–11.

https://doi.org/10.1037/xhp0001131

https://doi.org/10.1038/s41467-018-03029-x

Cuskley, C., & Kirby, S. (2013). Synesthesia, cross-modality, and language evolution. In J. Simner & E. Hubbard (Eds.), *Oxford handbook of synesthesia* (pp. 869–899). Oxford University Press. https://doi.org/10.5860/choice.50-5912

de Valk, J. M., Wnuk, E., Huisman, J. L. A., & Majid, A. (2017). Odor–color associations differ with verbal descriptors for odors: A comparison of three linguistically diverse groups. *Psychonomic Bulletin and Review*, *24*(4), 1171–1179. https://doi.org/10.3758/s13423-016-1179-2

Deroy, O., & Spence, C. (2013). Why we are not all synesthetes (not even weakly so). *Psychonomic Bulletin and Review*, *20*(4), 643–664. https://doi.org/10.3758/s13423-013-0387-2

Di Cicco, F., Van Zuijlen, M. J. P., Wijntjes, M. W. A., & Pont, S. C. (2021). Soft like velvet and shiny like satin: Perceptual material signatures of fabrics depicted in 17th century paintings. *Journal of Vision*, *21*(5), 1–22. https://doi.org/10.1167/JOV.21.5.10

Ernst, M. O. (2007). Learning to integrate arbitrary signals from vision and touch. *Journal of Vision*, *7*(5), 1–14. https://doi.org/10.1167/7.5.7

Essick, G. K., McGlone, F., Dancer, C., Fabricant, D., Ragin, Y., Phillips, N., Jones, T., & Guest, S. (2010). Quantitative assessment of pleasant touch. *Neuroscience and Biobehavioral Reviews*, *34*(2), 192–203. https://doi.org/10.1016/j.neubiorev.2009.02.003

Etzi, R., Spence, C., & Gallace, A. (2014). Textures that we like to touch: An experimental study of aesthetic preferences for tactile stimuli. *Consciousness and Cognition*, *29*, 178–188. https://doi.org/10.1016/j.concog.2014.08.011

Etzi, R., Spence, C., Zampini, M., & Gallace, A. (2016). When sandpaper is “kiki” and satin is "bouba": An exploration of the associations between words, emotional states, and the tactile attributes of everyday materials. *Multisensory Research*, *29*(1–3), 133–155. https://doi.org/10.1163/22134808-00002497

Faul, F., Erdfelder, E., Lang, A. G., & Buchner, A. (2007). G*Power 3: A flexible statistical power analysis program for the social, behavioral, and biomedical sciences. *Behavior Research Methods*, *39*(2), 175–191. https://doi.org/10.3758/BF03193146

Flanagan, J. R., Bittner, J. P., & Johansson, R. S. (2008). Experience can change distinct size-weight priors engaged in lifting objects and judging their weights. *Current Biology*, *18*(22), 1742–1747. https://doi.org/10.1016/j.cub.2008.09.042

Goubet, N., Durand, K., Schaal, B., & McCall, D. D. (2018). Seeing odors in color: Cross-modal associations in children and adults from two cultural environments. *Journal of Experimental Child Psychology*, *166*, 380–399. https://doi.org/10.1016/j.jecp.2017.09.007

Hein, G., Doehrmann, O., Müller, N. G., Kaiser, J., Muckli, L., & Naumer, M. J. (2007). Object familiarity and semantic congruency modulate responses in cortical audiovisual integration areas. *Journal of Neuroscience*, *27*(30), 7881–7887. https://doi.org/10.1523/JNEUROSCI.1740-07.2007

Huang, F., Wang, C., & Wan, X. (2022). Color-flavor interactions in associative learning: Evidence from a computerized matching task. *Food Quality and Preference*, *95*, 104364. https://doi.org/10.1016/j.foodqual.2021.104364

Ijzerman, H., Coan, J. A., Wagemans, F., Missler, M., Van Beest, I., Lindenberg, S., & Tops, M. (2015). A theory of social thermoregulation in human primates. *Frontiers in Psychology*, *6*, 1–17. https://doi.org/10.3389/fpsyg.2015.00464

Iosifyan, M. (2020). Crossmodal associations between cinema with elements of comic and tragic and texture touch. *Art and Perception*, *8*(2), 175–187. https://doi.org/10.1163/22134913-bja10004

Iosifyan, M., & Korolkova, O. (2019). Emotions associated with different textures during touch. *Consciousness and Cognition*, *71*, 79–85. https://doi.org/10.1016/j.concog.2019.03.012

Jaeger, S. R., Roigard, C. M., Jin, D., Vidal, L., & Ares, G. (2019). Valence, arousal and sentiment meanings of 33 facial emoji: Insights for the use of emoji in consumer research. *Food Research International*, *119*, 895–907. https://doi.org/10.1016/j.foodres.2018.10.074

Jaeger, S. R., Vidal, L., & Ares, G. (2021). Consumer product emotion research using emoji. In H. L. Meiselman (Ed.), *Emotion measurement* (2nd ed., pp. 535–558). Woodhead Publishing. https://doi.org/10.1016/b978-0-12-821124-3.00016-8

Kadosh, R. C., Henik, A., & Walsh, V. (2009). Synaesthesia: Learned or lost? *Developmental Science*, *12*(3), 484–491. https://doi.org/10.1111/j.1467-7687.2008.00798.x

Kaeppler, K. (2018). Crossmodal associations between olfaction and vision: Color and shape visualizations of odors. *Chemosensory Perception*, *11*(2), 95–111. https://doi.org/10.1007/s12078-018-9245-y

Kaliuzhna, M., Prsa, M., Gale, S., Lee, S. J., & Blanke, O. (2015). Learning to integrate contradictory multisensory self-motion cue pairings. *Journal of Vision*, *15*(1), 1–15. https://doi.org/10.1167/15.1.10

Kazak, A. E. (2018). Editorial: Journal article reporting standards. *American Psychologist*, *73*(1), 1–2. https://doi.org/10.1037/amp0000263

Kergoat, M., Giboreau, A., Nicod, H., Faye, P., Diaz, E., Beetschen, M. A., & Meyer, T. (2012). Consumer preference for tactile softness: A question of affect intensity? *Journal of Sensory Studies*, *27*(4), 232–246. https://doi.org/10.1111/j.1745-459X.2012.00388.x

https://doi.org/10.1037/xhp0001131

Klatzky, R. L., & Lederman, S. J. (2010). Multisensory texture perception. In M. J. Naumer & J. Kaiser (Eds.), *Multisensory object perception in the primate brain* (pp. 211–230). Springer. https://doi.org/10.1007/978-1-4419-5615-6_12

Knoeferle, K. M., Knoeferle, P., Velasco, C., & Spence, C. (2016). Multisensory brand search: How the meaning of sounds guides consumers' visual attention. *Journal of Experimental Psychology: Applied*, *22*(2), 196–210. https://doi.org/10.1037/xap0000084

Lähteenmäki, M., & Nummenmaa, L. (2015). Affective processing requires awareness. *Journal of Experimental Psychology: General*, *144*(2), 339–365. https://doi.org/10.1037/xge0000040.supp

Lenth, R. V. (2021). *emmeans: Estimated marginal means, aka least-squares means (version 1.7.0)* [R software package]. https://cran.r-project.org/package=emmeans

Lewkowicz, D. J., & Turkewitz, G. (1980). Cross-modal equivalence in early infancy: Auditory-visual intensity matching. *Developmental Psychology*, *16*(6), 597–607. https://doi.org/10.1037/0012-1649.16.6.597

Leys, C., Delacre, M., Mora, Y. L., Lakens, D., & Ley, C. (2019). How to classify, detect, and manage univariate and multivariate outliers, with emphasis on pre-registration. *International Review of Social Psychology*, *32*(1), 1–10. https://doi.org/10.5334/irsp.289

Leys, C., Ley, C., Klein, O., Bernard, P., & Licata, L. (2013). Detecting outliers: Do not use standard deviation around the mean, use absolute deviation around the median. *Journal of Experimental Social Psychology*, *49*(4), 764–766. https://doi.org/10.1016/j.jesp.2013.03.013

Liu, J., Lughofer, E., Zeng, X., & Li, Z. (2018). The power of visual texture in aesthetic perception: An exploration of the predictability of perceived aesthetic emotions. *Computational Intelligence and Neuroscience*, *2018*, 1812980.

https://doi.org/10.1155/2018/1812980

Lo, S., & Andrews, S. (2015). To transform or not to transform: Using generalized linear mixed models to analyse reaction time data. *Frontiers in Psychology*, *6*, 1171. https://doi.org/10.3389/fpsyg.2015.01171

Martino, G., & Marks, L. E. (1999). Perceptual and linguistic interactions in speeded classification: Tests of the semantic coding hypothesis. *Perception*, *28*(7), 903–923. https://doi.org/10.1068/p2866

Martino, G., & Marks, L. E. (2000). Cross-modal interaction between vision and touch: The role of synesthetic correspondence. *Perception*, *29*(6), 745–754. https://doi.org/10.1068/p2984

Martino, G., & Marks, L. E. (2001). Synesthesia: Strong and weak. *Current Directions in Psychological Science*, *10*(2), 61–65. https://doi.org/10.1111/1467-8721.00116

Motoyoshi, I., Nishida, S., Sharan, L., & Adelson, E. H. (2007). Image statistics and the perception of surface qualities. *Nature*, *447*(7141), 206–209. https://doi.org/10.1038/nature05724

Noelke, C., McGovern, M., Corsi, D. J., Jimenez, M. P., Stern, A., Wing, I. S., & Berkman, L. (2016). Increasing ambient temperature reduces emotional well-being. *Environmental Research*, *151*, 124–129. https://doi.org/10.1016/j.envres.2016.06.045

Novak, P. K., Smailović, J., Sluban, B., & Mozetič, I. (2015). Sentiment of emojis. *PLOS ONE*, *10*(12), e0144296. https://doi.org/10.1371/journal.pone.0144296

Palmer, S. E., Schloss, K. B., Xu, Z., & Prado-León, L. R. (2013). Music-color associations are mediated by emotion. *Proceedings of the National Academy of Sciences of the United States of America*, *110*(22), 8836–8841. https://doi.org/10.1073/pnas.1212562110

Parise, C. V. (2016). Crossmodal correspondences: Standing issues and experimental guidelines.

https://doi.org/10.1037/xhp0001131

Multisensory Research, *29*(1–3), 7–28. https://doi.org/10.1163/22134808-00002502

Parise, C. V., Knorre, K., & Ernst, M. O. (2014). Natural auditory scene statistics shapes human spatial hearing. *Proceedings of the National Academy of Sciences of the United States of America*, *111*(16), 6104–6108. https://doi.org/10.1073/pnas.1322705111

Parise, C. V., & Spence, C. (2012). Audiovisual crossmodal correspondences and sound symbolism: A study using the implicit association test. *Experimental Brain Research*, *220*(3–4), 319–333. https://doi.org/10.1007/s00221-012-3140-6

Parise, C. V., & Spence, C. (2013). Audiovisual cross-modal correspondences in the general population. In J. Simner & E. Hubbard (Eds.), *The Oxford handbook of synesthesia* (pp. 790–815). Oxford University Press. https://doi.org/10.1093/oxfordhb/9780199603329.013.0039

Partos, T. R., Cropper, S. J., & Rawlings, D. (2016). You don't see what I see: Individual differences in the perception of meaning from visual stimuli. *PLOS ONE*, *11*(3), e0150615. https://doi.org/10.1371/journal.pone.0150615

R Core Team. (2021). *R: A Language and Environment for Statistical Computing*. https://www.r-project.org/

Rimm-Kaufman, S. E., & Kagan, J. (1996). The psychological significance of changes in skin temperature. *Motivation and Emotion*, *20*(1), 63–78. https://doi.org/10.1007/BF02251007

Shams, L., & Seitz, A. R. (2008). Benefits of multisensory learning. *Trends in Cognitive Sciences*, *12*(11), 411–417. https://doi.org/10.1016/j.tics.2008.07.006

Signorell, A. (2021). *DescTools: Tools for descriptive statistics (version 0.99.43)* [R software package]. https://cran.r-project.org/package=DescTools

Smilek, D., Carriere, J. S. A., Dixon, M. J., & Merikle, P. M. (2007). Grapheme frequency and color luminance in grapheme-color synaesthesia. *Psychological Science*, *18*(9), 793–795. https://doi.org/10.1111/j.1467-9280.2007.01981.x

Spence, C. (2011). Crossmodal correspondences: A tutorial review. *Attention, Perception, & Psychophysics*, *73*(4), 971–995. https://doi.org/10.3758/s13414-010-0073-7

Spence, C. (2018). Crossmodal correspondences: A synopsis. In D. Howes (Ed.), *Senses and sensation: Critical and primary sources (Vol. 3)* (pp. 91–125). Bloomsbury Academic.

Spence, C. (2020a). Olfactory-colour crossmodal correspondences in art, science, and design. *Cognitive Research: Principles and Implications*, *5*(1), 1–21. https://doi.org/10.1186/s41235-020-00246-1

Spence, C. (2020b). Shitsukan—The multisensory perception of quality. *Multisensory Research*, *33*(7), 737–775. https://doi.org/10.1163/22134808-bja10003

Spence, C. (2020c). Temperature-based crossmodal correspondences: Causes and consequences. *Multisensory Research*, *33*(6), 1–38. https://doi.org/10.1163/22134808-20191494

Spence, C. (2022). Exploring group differences in the crossmodal correspondences. *Multisensory Research*, *35*(6), 495–536. https://doi.org/10.1163/22134808-bja10079

Spence, C., & Levitan, C. A. (2021). Explaining crossmodal correspondences between colours and tastes. *i-Perception*, *12*(3), 1–28. https://doi.org/10.1177/20416695211018223

Stevens, S. S. (1957). On the psychophysical law. *Psychological Review*, *64*(3), 153–181. https://doi.org/10.1037/h0046162

Teli, M. D. (2015). Softening finishes for textiles and clothing. In R. Paul (Ed.), *Functional finishes for textiles: Improving comfort, performance and protection* (pp. 123–152). Woodhead Publishing Limited. https://doi.org/10.1533/9780857098450.1.123

Toet, A., Kaneko, D., Ushiama, S., Hoving, S., Kruijf, I. de, Brouwer, A. M., Kallen, V., & van

https://doi.org/10.1037/xhp0001131

Erp, J. B. F. (2018). EmojiGrid: A 2D pictorial scale for the assessment of food elicited emotions. *Frontiers in Psychology*, *9*, 2396. https://doi.org/10.3389/fpsyg.2018.02396

Tsuda, H. (2020). *sketcher: An R package for converting a photo into a sketch style image (version 0.1.3)* [R software package]. https://cran.r-project.org/package=sketcher

Turoman, N., Velasco, C., Chen, Y. C., Huang, P. C., & Spence, C. (2018). Symmetry and its role in the crossmodal correspondence between shape and taste. *Attention, Perception, & Psychophysics*, *80*(3), 738–751. https://doi.org/10.3758/s13414-017-1463-x

Walker, P. (2016). Cross-sensory correspondences: A theoretical framework and their relevance to music. *Psychomusicology: Music, Mind, and Brain*, *26*(2), 103–116. https://doi.org/10.1037/pmu0000130

Walsh, V. (2003). A theory of magnitude: Common cortical metrics of time, space and quantity. *Trends in Cognitive Sciences*, *7*(11), 483–488. https://doi.org/10.1016/j.tics.2003.09.002

Wang, H., & Liu, L. (2020). Experimental investigation about effect of emotion state on people's thermal comfort. *Energy & Buildings*, *211*, 109789. https://doi.org/10.1016/j.enbuild.2020.109789

Witthoft, N., & Winawer, J. (2006). Synesthetic colors determined by having colored refrigerator magnets in childhood. *Cortex*, *42*(2), 175–183. https://doi.org/10.1016/S0010-9452(08)70342-3

Wongsriruksa, S., Howes, P., Conreen, M., & Miodownik, M. (2012). The use of physical property data to predict the touch perception of materials. *Materials and Design*, *42*, 238–244. https://doi.org/10.1016/j.matdes.2012.05.054

Zhang, D. (2017). A coefficient of determination for generalized linear models. *American Statistician*, *71*(4), 310–316. https://doi.org/10.1080/00031305.2016.1256839

Zhang, D. (2022). *rsq: R-Squared and Related Measures (version 2.5)* [R software package]. https://cran.r-project.org/package=rsq

Zhang, Y., & Risen, J. L. (2014). Embodied motivation: Using a goal systems framework to understand the preference for social and physical warmth. *Attitudes and Social Cognition, 107*(6), 965–977. https://doi.org/10.1037/a0038153